Extended periodic Anderson model close to a valence transition: A projector-based renormalization approach

Van-Nham Phan,[1,2] Alexander Mai,[1,3] and Klaus W. Becker[1]
[1]*Institut für Theoretische Physik, Technische Universität Dresden, D-01062 Dresden, Germany*
[2]*Institut für Physik, Ernst-Moritz-Arndt Universität Greifswald, D-17487 Greifswald, Germany*
[3]*Fachbereich Physik, Philipps-Universität Marburg, 35032 Marburg, Germany*
(Received 13 December 2009; revised manuscript received 13 May 2010; published 2 July 2010)

The one-dimensional periodic Anderson model with an additional Coulomb repulsion U_{fc} between localized f and conduction electrons has been investigated using the projector-based renormalization method. Due to the presence of U_{fc} and the hybridization V between localized and conduction electrons, various gaps are found in the quasiparticle dispersion $\tilde{\varepsilon}_k$. The number of gaps depends on the density of the localized electrons. Moreover, a valence transition from an integer to a mixed f valence is found as a function of the bare f level energy $\bar{\varepsilon}_f$. Its dependence on various model parameters is investigated for fixed total electron density. In particular, the transition is sharpened either by increasing U_{fc} or by decreasing the hybridization or the temperature.

DOI: 10.1103/PhysRevB.82.045101 PACS number(s): 71.10.Fd, 71.27.+a, 75.30.Mb

I. INTRODUCTION

The observation of a superconducting phase in $CeCu_2Si_2$ and related heavy-fermion compounds under high external pressure[1,2] yields a new possibility to study the mechanism of unconventional superconductivity. At small applied pressure (≤ 1 GPa), a small superconducting dome is found close to an antiferromagnetic phase.[3] It is believed that the superconducting pairing is mediated by spin fluctuations[4–6] in this case. Upon further increasing the pressure, a second superconducting dome with a higher critical temperature appears.[1,2] In this regime, the residual resistivity ρ_0 exhibits a peaklike behavior as a function of pressure and the coefficient A of the T^2 term of the resistivity rapidly decreases with increasing pressure.[2] As it is known for heavy-fermion systems in the Kondo limit $n_f \approx 1$, the quantity $\sqrt{A}$ scales as $m^*/m=(1-n_f/2)/(1-n_f)$,[7] where n_f is the f occupation number of the Ce ions and m^* is the effective mass of the quasiparticles. Therefore, the rapid decrease in A is related to a sharp change in the Ce valence. It is claimed[8] that the increase in the residual resistivity ρ_0 can be understood as a many-particle effect that enhances the impurity potential. The quantity ρ_0 is also proportional to the valence susceptibility $-(\partial n_f/\partial \bar{\varepsilon}_f)_\mu$, where $\bar{\varepsilon}_f$ is the bare atomic f level of the Ce ion and μ is the chemical potential.[8] Thus, the enhancement of ρ_0 can be directly related to the sharpness of the valence change. Another hint, that valence fluctuations may enhance the superconducting critical temperature, is a rapid volume change, which is observed by x-ray diffraction in $CeCu_2Ge_2$ at cryogenic temperature[9] for the same pressure $P \sim P_v$ at which the second superconducting dome is found. Therefore, the investigation of the valence instability is important for the understanding of superconductivity in heavy-fermion systems.

The abrupt change in the valence of Ce ions in heavy-fermion systems under high pressure was qualitatively described in Ref. 10 by including a large Coulomb repulsion U_{fc} between localized f and conduction electrons in the periodic Anderson model (PAM). Investigating this so-called extended PAM (EPAM) in three dimensions using a slave-boson mean-field approximation, it was found that valence fluctuations, which occur if the bare f electron level $\bar{\varepsilon}_f$ is tuned relative to the Fermi level, are considerably enhanced by a moderate strength of U_{fc}.[11] Associated with the rapid valence change, d-wave superconductivity was found, and the authors pointed out that superconductivity may be caused by valence fluctuations. The valence instability was also studied for the one-dimensional (1D) extended PAM (Ref. 12) using the density-matrix renormalization group (DMRG). However, it occurred only if U_{fc} was larger than the conduction electron bandwidth and the f electron energy $\bar{\varepsilon}_f$ was located below the conduction band. In this treatment superconducting singlet pairing was dominant in the valence transition regime.

Recently, the EPAM was also studied using dynamical mean-field theory.[13] The results are in good agreement with the DMRG calculations. Also the two-dimensional EPAM was investigated by applying the fluctuation-exchange approximation. It was found that for modest U_{fc} the system is unstable toward a charge-density wave, which may also lead to superconductivity.[14] Thus, at present, it is still unclear whether superconductivity in the EPAM due to the valence fluctuations occurs only for strong couplings U_{fc} or also in the weak-coupling regime. Therefore, alternative theoretical approaches are desirable to further study this problem.

In this paper, we investigate the physical properties of the EPAM in the valence transition regime using a recently developed many-particle method called projector-based renormalization method (PRM).[15] Note that we do not concentrate on the Kondo regime where the typical heavy-fermion behavior is found. Therefore, the physical behavior of the Kondo lattice[16] as a limiting case of the PAM is not contained in the present treatment. Also, the discussion of a possible superconducting phase in the valence transition regime will be postponed to a forthcoming paper. The projector-based renormalization method is based on the derivation of a renormalized diagonal or quasidiagonal Hamiltonian by the repeated application of unitary transformations. The method was already used before to study the valence transition in the usual PAM.[17] There, in the case of fixed

chemical potential, a drastic change in the f occupation from an integral to a mixed valence was observed. This transition can be understood as a crossing of the renormalized f level from below to above the Fermi level. Due to the presence of strong electronic correlations, various approximations had to be applied in this treatment. In particular, no solutions could be found for a f level degeneracy of $\nu_f=2$. To overcome this restriction and to simplify the renormalization procedure, in the present approach we employ a more general version of the PRM, which is based on a better choice of the generator of the unitary transformation for this case.[18,19] As a consequence, the renormalization equations for the parameters of the Hamiltonian are differential equations instead of difference equations as in the former approach.

The paper is organized as follows. In Sec. II, we introduce the EPAM. Section III introduces the PRM. Its application to the EPAM is presented in Sec. IV. In Sec. V, the numerical solution for the renormalization equations is given. Also, the electronic dispersion and the dependence of the valence transition on the various model parameters is discussed. The last section contains our conclusions.

II. EXTENDED PERIODIC ANDERSON MODEL

The EPAM is given by the Hamiltonian,

$$\mathcal{H} = (\bar{\varepsilon}_f - \mu)\sum_{i,m} f_{im}^{\dagger} f_{im} + \sum_{\mathbf{k},m} (\bar{\varepsilon}_{\mathbf{k}} - \mu) c_{\mathbf{k}m}^{\dagger} c_{\mathbf{k}m} + \frac{1}{\sqrt{N}} \sum_{\mathbf{k},i,m} V_{\mathbf{k}} (f_{im}^{\dagger} c_{\mathbf{k}m} e^{i\mathbf{k}\mathbf{R}_i} + \text{H.c.}) + U_{fc} \sum_{i,mm'} n_{im}^{c} n_{im'}^{f} + U_f \sum_{i,m\neq m'} n_{im}^{f} n_{im'}^{f}. \quad (1)$$

Here, $f_{im}^{\dagger}(f_{im})$ and $c_{\mathbf{k}m}^{\dagger}$ $(c_{\mathbf{k}m})$ are creation (annihilation) operators of f electrons at site i and of conduction electrons with wave vector $\mathbf{k}$, respectively. Angular momentum and spin indices are combined in one index m (of degeneracy ν_f) which is assumed to be equal for f and c electrons for simplicity. The bare energies of f and conduction electrons are denoted by $\bar{\varepsilon}_f$ and $\bar{\varepsilon}_{\mathbf{k}}$. The chemical potential μ can be used to adjust the total electron density and N is the number of lattice sites. The hybridization $V_{\mathbf{k}}$ between localized and delocalized electrons is described by the third term of Eq. (1). In general, $V_{\mathbf{k}}$ may depend on the wave vector $\mathbf{k}$.[20,21] However, for simplicity a $\mathbf{k}$-independent V will be used in the following. The last two terms represent the local Coulomb repulsion U_f between the f electrons and between the f and the conduction electrons (U_{fc}). Since $U_f \gg U_{fc}$, we assume U_f to be infinite. Hence, f sites can either be empty or singly occupied. The exclusion of double occupied f sites is realized by introducing Hubbard operators (often also called X operators[22])

$$\hat{f}_{im}^{\dagger} = f_{im}^{\dagger} \prod_{\tilde{m}(\neq m)} (1 - f_{i\tilde{m}}^{\dagger} f_{i\tilde{m}}) =: f_{im}^{\dagger} D_{im}, \quad (2)$$

which replace the usual f operators. Here the operator D_{im} is a local projection operator onto the empty f state at site i and the singly occupied state with angular momentum m. Note that the Hubbard operators do not obey the usual fermionic anticommutation relations but instead

$$[\hat{f}_{im}^{\dagger}, \hat{f}_{im'}]_+ = \delta_{m,m'} D_{im}, \quad (3)$$

where an additional spin-flip term on the right-hand side for $m \neq m'$ will be neglected from the beginning. The inclusion of such a term would be necessary for a proper treatment of the Kondo regime, as will be explained below.

To simplify our calculation, we introduce local fluctuation operators

$$\delta(n_{im}^{c}) = n_{im}^{c} - \langle n_{im}^{c} \rangle, \quad \delta(\hat{n}_{im'}^{f}) = \hat{n}_{im'}^{f} - \langle \hat{n}_{im'}^{f} \rangle \quad (4)$$

and use the identity

$$n_{im}^{c} \hat{n}_{im'}^{f} = n_{im}^{c} \langle \hat{n}_{im'}^{f} \rangle + \hat{n}_{im'}^{f} \langle n_{im}^{c} \rangle + \langle n_{im}^{c} \rangle \langle \hat{n}_{im'}^{f} \rangle + \delta(n_{im}^{c}) \delta(\hat{n}_{im'}^{f}). \quad (5)$$

Hence, in the limit $U_f \to \infty$, we can write

$$\mathcal{H} = \varepsilon_f \sum_{i,m} \hat{f}_{im}^{\dagger} \hat{f}_{im} + \sum_{\mathbf{k},m} \varepsilon_{\mathbf{k}} c_{\mathbf{k}m}^{\dagger} c_{\mathbf{k}m} + \frac{1}{\sqrt{N}} \sum_{\mathbf{k},i,m} V (\hat{f}_{im}^{\dagger} c_{\mathbf{k}m} e^{i\mathbf{k}\mathbf{R}_i} + \text{H.c.}) + U_{fc} \sum_{i,mm'} \delta(n_{im}^{c}) \delta(\hat{n}_{im'}^{f}) - U_{fc} N \langle n^{c} \rangle \langle \hat{n}^{f} \rangle, \quad (6)$$

where

$$\varepsilon_f = \bar{\varepsilon}_f + U_{fc} \langle n^{c} \rangle - \mu, \quad \varepsilon_{\mathbf{k}} = \bar{\varepsilon}_{\mathbf{k}} + U_{fc} \langle \hat{n}^{f} \rangle - \mu. \quad (7)$$

The influence of U_{fc} on valence transitions was first studied in the single impurity Anderson model.[23] Here, using a mean-field approximation, a discontinuous transition was found for a large value of U_{fc}. For the periodic model, the effect of U_{fc} on valence fluctuations was discussed using Hartree-Fock-type approximations, slave-boson mean-field approximations[24,25] and large-N expansions.[11] All these approaches showed that a large U_{fc} leads to a rapid change in the average f electron occupation when the f level $\bar{\varepsilon}_f$ is varied.

Without U_{fc}, the model (6) was successfully solved by the PRM in order to investigate the valence transition for fixed chemical potential.[17,18] There, in the case of small values of ν_f, the f occupation drastically changed showing a sudden breakdown of the state with integral f occupation to a mixed-valence state. On the other hand, without the hybridization term, Hamiltonian (6) describes the one-dimensional Falicov-Kimball model (FKM), which has also been studied using the PRM.[26] Remarkably, at low temperatures, a gap in the electronic quasiparticle dispersion appears due to the presence of the Coulomb repulsion U_{fc}. In the present work, the PRM is applied to the EPAM, Eq. (6), where both a Coulomb repulsion U_{fc} and a hybridization V between the localized and the conduction electrons is present. Therefore, gaps in the quasiparticle spectrum of the conduction electrons are expected not only due to the Coulomb repulsion but also due to the hybridization.

III. PROJECTOR-BASED RENORMALIZATION METHOD

In this section, we give a short introduction to the PRM. In some aspects, this approach resembles Wegner's flow

equation method[27] and also the similarity renormalization by Głazek and Wilson.[28,29] The PRM was introduced[15] as an alternative approach to many-particle systems and was already applied to a number of different systems. Examples are the investigation of phonon-mediated superconductivity starting from an explicit expression for the electron-phonon interaction[30] and the discussion of the metal-insulator transition in the Holstein model.[31] Many-particle systems in the presence of strong correlations such as the PAM were also investigated.[32] In contrast to the slave-boson mean-field treatment,[33] the PRM maps the periodic Anderson model onto an effective model of two independent subsystems of renormalized conduction and f electrons, thereby still taking into account the strong correlations between the localized f electrons. Mixed and integral valent solutions for the f electrons were found.[17] As a slight modification of the original PRM version, a somewhat changed generator for the unitary transformation can be used in the case of the periodic Anderson model. Thereby, the originally stepwise unitary transformation was replaced by a continuous one leading to differential renormalization equations.[18,19] This is useful for applying existing computer subroutines for solving the renormalization equations numerically.

The PRM starts from the separation of a given many-particle Hamiltonian, $\mathcal{H}=\mathcal{H}_0+\mathcal{H}_1$. Thereby, it is assumed that the eigenvalues $E_n^{(0)}$ and eigenvectors $|n\rangle$ of the dominant part $\mathcal{H}_0$ are known,

$$\mathcal{H}_0|n\rangle = E_n^{(0)}|n\rangle. \tag{8}$$

The interaction $\mathcal{H}_1$ is chosen to have no diagonal matrix elements with respect to the eigenvectors of $\mathcal{H}_0$, i.e., $\langle n|\mathcal{H}_1|m\rangle \neq 0$. The presence of $\mathcal{H}_1$ usually prevents an exact solution of the full Hamiltonian $\mathcal{H}$.

The goal of the PRM is to transform the initial Hamiltonian into an effective Hamiltonian $\mathcal{H}_\lambda$ which has no transition matrix elements with energy differences greater than some chosen cutoff $\lambda < \Lambda$. Here, Λ is the largest transition energy in the original model. The Hamiltonian $\mathcal{H}_\lambda$ is determined by a unitary transformation according to

$$\mathcal{H}_\lambda = e^{X_\lambda}\mathcal{H}e^{-X_\lambda}, \tag{9}$$

which can again be decomposed,

$$\mathcal{H}_\lambda = \mathcal{H}_{0,\lambda} + \mathcal{H}_{1,\lambda}. \tag{10}$$

$\mathcal{H}_{1,\lambda}$ is constructed so that all matrix elements with an energy difference $|E_n^\lambda - E_m^\lambda| > \lambda$ vanish, $\langle n_\lambda|\mathcal{H}_{1,\lambda}|m_\lambda\rangle = 0$, where E_n^λ and $|n_\lambda\rangle$ are the new eigenvalues and eigenstates of $\mathcal{H}_{0,\lambda}$. Note that in the framework of the PRM, neither $|n_\lambda\rangle$ nor $|m_\lambda\rangle$ have to be low-energy eigenstates of $\mathcal{H}_{0,\lambda}$. The unitary transformation, Eq. (9), guarantees that the Hamiltonian $\mathcal{H}_\lambda$ has the same eigenspectrum as $\mathcal{H}$. To ensure the hermiticity of $\mathcal{H}_\lambda$, the generator X_λ of the unitary transformation satisfies $X_\lambda^\dagger = -X_\lambda$.

In the PRM, a crucial idea of the elimination of the transition matrix elements is carried out by defining projection operators

$$\mathbf{P}_\lambda \mathcal{A} = \sum_{\substack{m,n \\ |E_n^\lambda - E_m^\lambda| \leq \lambda}} |n_\lambda\rangle\langle m_\lambda|\langle n_\lambda|\mathcal{A}|m_\lambda\rangle. \tag{11}$$

Note that $\mathbf{P}_\lambda$ is a superoperator acting on ordinary operators $\mathcal{A}$ of the Hilbert space of the system. Therefore, $\mathbf{P}_\lambda$ can be interpreted as a projection operator in the Liouville space that is built up of all operators of the Hilbert space. Note that in Eq. (11) only states $|n_\lambda\rangle$ and $|m_\lambda\rangle$ satisfying $|E_n^\lambda - E_m^\lambda| \leq \lambda$ contribute. The orthogonal complement of $\mathbf{P}_\lambda$, $\mathbf{Q}_\lambda = 1 - \mathbf{P}_\lambda$, projects onto the high-energy transitions of $\mathcal{A}$. To find an appropriate generator X_λ of the unitary transformation, we employ the condition that the matrix elements for transitions of $\mathcal{H}_\lambda$ with energy differences larger than λ vanish, i.e., the condition

$$\mathbf{Q}_\lambda \mathcal{H}_\lambda = 0 \tag{12}$$

must be fulfilled.

With the chosen generator X_λ, the Hamiltonian $\mathcal{H}_\lambda$ can be evaluated by Eq. (9). It is convenient to perform the elimination procedure stepwise so that each step reduces the cutoff energy λ by a small amount $\Delta\lambda$. Thus, starting at the initial cutoff Λ of the Hamiltonian, after the first step, all transitions with energy transfers between Λ and $\Lambda - \Delta\lambda$ are removed. The subsequent steps remove all transitions larger than $\Lambda - \Delta\lambda$, $\Lambda - 2\Delta\lambda$, and so on. The unitary transformation for the step from an intermediate cutoff λ to a new cutoff $\lambda - \Delta\lambda$ can be evaluated using

$$\mathcal{H}_{\lambda-\Delta\lambda} = e^{X_{\lambda,\Delta\lambda}}\mathcal{H}_\lambda e^{-X_{\lambda,\Delta\lambda}}, \tag{13}$$

where the generator $X_{\lambda,\Delta\lambda}$ is fixed by

$$\mathbf{Q}_{\lambda-\Delta\lambda}\mathcal{H}_{\lambda-\Delta\lambda} = 0, \tag{14}$$

in analogy to Eq. (9). This condition ensures that $\mathcal{H}_{\lambda-\Delta\lambda}$ has no matrix elements connecting eigenstates of $\mathcal{H}_{0,\lambda-\Delta\lambda}$ with energy differences larger than $\lambda - \Delta\lambda$.

The generator $X_{\lambda,\Delta\lambda}$ is not completely fixed by Eqs. (13) and (14). In fact, the part $\mathbf{P}_{\lambda-\Delta\lambda}X_{\lambda,\Delta\lambda}$ associated with the low-energy excitations can still be chosen arbitrarily and, in principle, physical results derived from the renormalization scheme should not depend on any particular choice of that part. However, in practice, a particular choice of $\mathbf{P}_{\lambda-\Delta\lambda}X_{\lambda,\Delta\lambda}$ can be important. If $\mathbf{P}_{\lambda-\Delta\lambda}X_{\lambda,\Delta\lambda}=0$ is chosen, the minimal transformation to match requirement, Eq. (14), is performed. This choice has been used in the discrete version of the PRM.[17,19] However, in particular cases a nonzero choice for $\mathbf{P}_{\lambda-\Delta\lambda}X_{\lambda,\Delta\lambda}$ might help to circumvent problems in the numerical evaluation of the renormalization equations. In the continuous version of the PRM,[19] a nonzero $\mathbf{P}_{\lambda-\Delta\lambda}X_{\lambda,\Delta\lambda}$ is allowed and the generator $X_{\lambda,\Delta\lambda}$ can be written as follows:

$$X_{\lambda,\Delta\lambda} = \mathbf{P}_{\lambda-\Delta\lambda}X_{\lambda,\Delta\lambda} + \mathbf{Q}_{\lambda-\Delta\lambda}X_{\lambda,\Delta\lambda}. \tag{15}$$

Here the part $\mathbf{Q}_{\lambda-\Delta\lambda}X_{\lambda,\Delta\lambda}$ ensures that Eq. (14) is fulfilled. An appropriate choice of the remaining part $\mathbf{P}_{\lambda-\Delta\lambda}X_{\lambda,\Delta\lambda}$ is fixed in such a way that it almost completely eliminates all interaction parameters before the cutoff energy λ is reached. In this case, even the part $(\mathbf{Q}_{\lambda-\Delta\lambda}X_{\lambda,\Delta\lambda})$ can be neglected at all.

Note that in general, new interaction terms will be generated in each renormalization step. This might allow the in-

vestigation of competing interactions which naturally emerge in the renormalization procedure. Actual calculations require a closed set of renormalization equations. Therefore, the originally chosen operator structure of $\mathcal{H}_\lambda$ must be kept during the renormalization procedure and factorizations must be used to truncate higher-order operator terms. Consequently, an initially chosen ansatz for $\mathcal{H}_\lambda$ might be limited to a certain parameter regime, if important operators for a different regime have not been included.

Due to the factorization approximation, the renormalization equations still contain expectation values which must be calculated separately. In principle, they are defined with $\mathcal{H}_\lambda$ since the factorization approximation was employed for the renormalization step from $\mathcal{H}_\lambda$ to $\mathcal{H}_{\lambda-\Delta\lambda}$. However, $\mathcal{H}_\lambda$ always contains interactions which prevent a straightforward evaluation. The easiest way to circumvent this difficulty would be to neglect all interactions and use the diagonal part $\mathcal{H}_{0,\lambda}$ instead of the full $\mathcal{H}_\lambda$. This approach was successfully applied for the single-particle excitations and the phonon softening close to the metal-insulator transition in the half-filled Holstein model.[34] However, it turned out that often the interaction terms in $\mathcal{H}_\lambda$ are crucial for a proper calculation of the required expectation values. Therefore, in the following we shall include interaction effects by evaluating the expectation values with the full Hamiltonian $\mathcal{H}$ instead of $\mathcal{H}_\lambda$. In this case, the solution of the renormalization equations requires an additional self-consistency loop that guarantees the correct result for the expectation values.

One way to evaluate the expectation values starts from the free energy which can be calculated either from the original $\mathcal{H}$ or from the renormalized Hamiltonian $\tilde{\mathcal{H}}=\lim_{\lambda\to 0}\mathcal{H}_\lambda$,

$$F=-\frac{1}{\beta}\ln \mathrm{Tr}\, e^{-\beta\mathcal{H}}=-\frac{1}{\beta}\ln \mathrm{Tr}\, e^{-\beta\tilde{\mathcal{H}}}, \tag{16}$$

since $\tilde{\mathcal{H}}$ is obtained from $\mathcal{H}$ by a unitary transformation. The desired expectation values can then be determined from the free energy by functional derivatives.[30,32]

The second way employs an additional unitary transformation for the operator variable $\mathcal{A}$, for which the expectation value is evaluated,

$$\langle\mathcal{A}\rangle=\frac{\mathrm{Tr}(\mathcal{A}e^{-\beta\mathcal{H}})}{\mathrm{Tr}\, e^{-\beta\mathcal{H}}}=\frac{\mathrm{Tr}(\tilde{\mathcal{A}}e^{-\beta\tilde{\mathcal{H}}})}{\mathrm{Tr}\, e^{-\beta\tilde{\mathcal{H}}}}. \tag{17}$$

Here we have defined $\tilde{\mathcal{A}}=\lim_{\lambda\to 0}\mathcal{A}_\lambda$, where $\mathcal{A}_\lambda=e^{X_\lambda}\mathcal{A}e^{-X_\lambda}$. Therefore, additional renormalization equations need to be derived for the λ-dependent operator $\mathcal{A}_\lambda$.

The formal way to find the equations for $\mathcal{H}_\lambda$ and similarly for $\mathcal{A}_\lambda$ is to compare the λ-dependent coefficients in the renormalization ansatz, Eq. (10), for $\mathcal{H}_\lambda$ at cutoff $\lambda-\Delta\lambda$ with those of the explicitly evaluated expression Eq. (13). The obtained difference equations for the parameters reduce to differential equations for $\Delta\lambda\to 0$. Finally, in the step $\lambda\to 0$, the fully renormalized Hamiltonian $\mathcal{H}_{\lambda\to 0}=\mathcal{H}_{0,\lambda\to 0}$ is obtained and the interaction Hamiltonian $\mathcal{H}_1$ completely vanishes, $\mathcal{H}_{1,\lambda\to 0}=0$. Note that the coefficients in the fully renormalized Hamiltonian depend on the initial parameter values of the original model.

The PRM is based on the general idea that interaction terms of a many-particle system $\mathcal{H}$ are eliminated by unitary transformations. The approach removes high-energy transitions but does not reduce the Hilbert space. This is different from the poor man's scaling[35] which removes high-energy states so that the Hilbert space is reduced. The similarity transformation of Wilson[28,29] and also Wegner's flow equation method[27] start from *continuous* transformations in differential form. In contrast, in its original form, the PRM is based on *discrete* transformations which lead to coupled difference equations. This allows a unified treatment of quantum phase transition on both sides of a critical point.[31] In the present investigation an extension of the PRM to continuous transformations will be used which is the better choice for the periodic Anderson model.

IV. RENORMALIZATION OF THE EPAM

A. Generator of the unitary transformation

In order to derive renormalization equations for the parameters of the Hamiltonian, we have to start from the generator of the unitary transformation, Eq. (13). An approximate expression for the generator X_λ will be constructed on the basis of the continuous transformation idea discussed in the last section. The Hamiltonian of the EPAM, Eq. (6), can be decomposed into

$$\mathcal{H}_0=\varepsilon_f\sum_{i,m}\hat{f}^\dagger_{im}\hat{f}_{im}+\sum_{\mathbf{k},m}\varepsilon_{\mathbf{k}}c^\dagger_{\mathbf{k}m}c_{\mathbf{k}m}-U_{fc}N\langle n^c\rangle\langle\hat{n}^f\rangle \tag{18}$$

and

$$\mathcal{H}_1=\frac{1}{\sqrt{N}}\sum_{\mathbf{k},i,m}V(\hat{f}^\dagger_{im}c_{\mathbf{k}m}e^{i\mathbf{k}\mathbf{R}_i}+\mathrm{H.c.})+U_{fc}\sum_{\mathbf{kq},m}a_{\mathbf{k},\mathbf{k}+\mathbf{q},m} \tag{19}$$

with

$$a_{\mathbf{k},\mathbf{k}+\mathbf{q},m}=\frac{1}{N}\delta(c^\dagger_{\mathbf{k}m}c_{\mathbf{k}+\mathbf{q},m})\sum_{i,m'}\delta(\hat{f}^\dagger_{im'}\hat{f}_{im'})e^{-i\mathbf{q}\mathbf{R}_i}. \tag{20}$$

Apart from the hybridization, the perturbation $\mathcal{H}_1$ contains the fluctuating part of the Coulomb repulsion U_{fc}. In principle, the latter operator could be factorized also into a hybridizationlike operator contribution $\langle c^\dagger_{\mathbf{k}m}\hat{f}_{im}\rangle\hat{f}^\dagger_{im}c_{\mathbf{k}m}+\mathrm{H.c.}$ However, the local density operator $\hat{f}^\dagger_{im}\hat{f}_{im}$ would thereby be factorized which should be avoided since the local constraints imposed by Hubbard operators would be violated in this case. Products of Hubbard operators at the same local site should always be kept as entities in order to obey the influence of the strong electronic correlations.

To obtain the operator structure of X_λ, we consider the following ansatz for the generator,

$$X_\lambda\sim\frac{1}{\mathcal{L}_0}\mathcal{H}_1,$$

which is motivated by perturbation theory.[15] Here $\mathcal{L}_0$ is the unperturbed Liouville operator that is defined by $\mathcal{L}_0A=[\mathcal{H}_0,A]$ for any operator A. For the operators $a_{\mathbf{k},\mathbf{k}+\mathbf{q},m}$ and $\hat{f}^\dagger_{\mathbf{k}m}c_{\mathbf{k}m}$ in Eq. (19), we obtain

$$\mathcal{L}_0 a_{\mathbf{k},\mathbf{k}+\mathbf{q},m} = (\varepsilon_{\mathbf{k}} - \varepsilon_{\mathbf{k}+\mathbf{q}}) a_{\mathbf{k},\mathbf{k}+\mathbf{q},m},$$

$$\mathcal{L}_0 \hat{f}^{\dagger}_{\mathbf{k}m} c_{\mathbf{k}m} = (\varepsilon_f - \varepsilon_{\mathbf{k}}) \hat{f}^{\dagger}_{\mathbf{k}m} c_{\mathbf{k}m}.$$

Hence, they can be interpreted as eigenoperators of the Liouville operator $\mathcal{L}_0$ and the generator X_λ to first order has the form

$$X_\lambda = \sum_{\mathbf{k},\mathbf{q},m} \mathcal{U}_{\mathbf{k},\mathbf{k}+\mathbf{q},\lambda} a_{\mathbf{k},\mathbf{k}+\mathbf{q},m} + \sum_{\mathbf{k},m} \mathcal{V}_{\mathbf{k},\lambda} (\hat{f}^{\dagger}_{\mathbf{k}m} c_{\mathbf{k}m} - \text{H.c.}) \tag{21}$$

with some prefactors $\mathcal{U}_{\mathbf{k},\mathbf{k}+\mathbf{q},\lambda}$ and $\mathcal{V}_{\mathbf{k},\lambda}$. Using this generator for the unitary transformation, Eq. (9), we can derive an appropriate ansatz for the renormalized Hamiltonian $\mathcal{H}_\lambda$ after all excitations with energies larger than cutoff λ have been eliminated. It is given by

$$\mathcal{H}_\lambda = \mathcal{H}_{0,\lambda} + \mathcal{H}_{1,\lambda} \tag{22}$$

with

$$\mathcal{H}_{0,\lambda} = N\varepsilon_{f,\lambda} \sum_m (\hat{f}^{\dagger}_m \hat{f}_m)_{\text{L}} + \sum_{\mathbf{k},m} \gamma_{\mathbf{k},\lambda} (\hat{f}^{\dagger}_{\mathbf{k}m} \hat{f}_{\mathbf{k}m})_{\text{NL}} + \sum_{\mathbf{k},m} \varepsilon_{\mathbf{k},\lambda} c^{\dagger}_{\mathbf{k}m} c_{\mathbf{k}m} + \sum_{\substack{i,j\neq i \\ mm'}} g_{ij,\lambda} \delta\hat{n}^f_{im} \delta\hat{n}^f_{jm'} + E_\lambda \tag{23}$$

and

$$\mathcal{H}_{1,\lambda} = \mathbf{P}_\lambda \mathcal{H}_1 = \mathbf{P}_\lambda \sum_{\mathbf{k},m} V_{\mathbf{k},\lambda} (\hat{f}^{\dagger}_{\mathbf{k}m} c_{\mathbf{k}m} + \text{H.c.}) + \mathbf{P}_\lambda \sum_{\mathbf{k},\mathbf{q},m} U_{\mathbf{k},\mathbf{k}+\mathbf{q},\lambda} a_{\mathbf{k},\mathbf{k}+\mathbf{q},m}. \tag{24}$$

Here, $\mathbf{P}_\lambda$ is a projection operator in the Liouville space. It projects onto all low-energy transitions with energies smaller than λ with respect to the unperturbed Hamiltonian $\mathcal{H}_{0,\lambda}$. Note that all prefactors in Eq. (22) now depend on the cutoff λ. Moreover, additional terms have been generated. Besides an energy shift E_λ, also a new interaction term $\sim g_{ij,\lambda}$ between the localized f electron densities appears in $\mathcal{H}_{0,\lambda}$ and an additional hopping between different f sites. Here

$$(\hat{f}^{\dagger}_{\mathbf{k}m} \hat{f}_{\mathbf{k}m})_{\text{NL}} = \frac{1}{N} \sum_{i\neq j} \hat{f}^{\dagger}_{im} \hat{f}_{jm} e^{i\mathbf{k}(\mathbf{R}_i - \mathbf{R}_j)} \tag{25}$$

is the nonlocal (NL) part of the k-dependent f electron density operator, whereas the local part is given by

$$(\hat{f}^{\dagger}_m \hat{f}_m)_{\text{L}} = \frac{1}{N} \sum_{\mathbf{k}} \hat{f}^{\dagger}_{\mathbf{k}m} \hat{f}_{\mathbf{k}m} = \frac{1}{N} \sum_i \hat{f}^{\dagger}_{im} \hat{f}_{im}. \tag{26}$$

Both parts obey the simple relation

$$(\hat{f}^{\dagger}_{\mathbf{k}m} \hat{f}_{\mathbf{k}m})_{\text{NL}} + (\hat{f}^{\dagger}_m \hat{f}_m)_{\text{L}} = \hat{f}^{\dagger}_{\mathbf{k}m} \hat{f}_{\mathbf{k}m}. \tag{27}$$

Finally, $\hat{f}^{\dagger}_{\mathbf{k}m}$ is the Fourier transform of $\hat{f}^{\dagger}_{im}$,

$$\hat{f}^{\dagger}_{\mathbf{k}m} = \frac{1}{\sqrt{N}} \sum_i \hat{f}^{\dagger}_{im} e^{i\mathbf{k}\mathbf{R}_i}. \tag{28}$$

The initial parameter values at the cutoff Λ of the original model are

$$\varepsilon_{f,\Lambda} = \varepsilon_f, \quad g_{ij,\Lambda} = 0, \quad \gamma_{\mathbf{k},\Lambda} = 0, \quad V_{\mathbf{k},\Lambda} = V,$$

$$\varepsilon_{\mathbf{k},\Lambda} = \varepsilon_{\mathbf{k}}, \quad U_{\mathbf{k},\mathbf{k}+\mathbf{q},\Lambda} = U_{fc}, \quad E_\Lambda = -NU_{fc} \langle n^c \rangle \langle \hat{n}^f \rangle. \tag{29}$$

Next, we have to evaluate the action of the superoperator $\mathbf{P}_\lambda$ on the interaction operators in $\mathcal{H}_\lambda$ to fulfill the requirement $\mathbf{Q}_\lambda \mathcal{H}_\lambda = 0$. First we apply the unperturbed Liouville operator $\mathcal{L}_{0,\lambda}$ at cutoff λ to $\hat{f}^{\dagger}_{\mathbf{k}m} c_{\mathbf{k}m}$ and to $a_{\mathbf{k},\mathbf{k}+\mathbf{q},m}$ in order to find the excitation energies of the renormalized Hamiltonian $\mathcal{H}_{1,\lambda}$. The resulting eigenvalues of $\mathcal{L}_{0,\lambda}$ can be understood as excitation energies caused by the hybridization and the Coulomb interaction. Let us first consider the hybridization term

$$\begin{aligned} \mathcal{L}_{0,\lambda} \hat{f}^{\dagger}_{\mathbf{k}m} c_{\mathbf{k}m} &= (\varepsilon_{f,\lambda} - \varepsilon_{\mathbf{k},\lambda}) \hat{f}^{\dagger}_{\mathbf{k}m} c_{\mathbf{k}m} \\ &+ \frac{1}{N^{3/2}} \sum_{\mathbf{p},i,j} (1 - \delta_{ij}) \gamma_{\mathbf{p},\lambda} \hat{f}^{\dagger}_{im} D_{jm} c_{\mathbf{k}m} e^{i(\mathbf{k}-\mathbf{p})\mathbf{R}_j} e^{i\mathbf{p}\mathbf{R}_i} \\ &+ \frac{1}{N^{3/2}} \sum_{\mathbf{p},i,j,m'} (1 - \delta_{mm'}) \\ &\times \gamma_{\mathbf{p},\lambda} \hat{f}^{\dagger}_{im} \hat{f}^{\dagger}_{jm} \hat{f}_{jm'} c_{\mathbf{k}m} e^{i(\mathbf{k}-\mathbf{p})\mathbf{R}_j} e^{i\mathbf{p}\mathbf{R}_i}, \end{aligned} \tag{30}$$

where the second and third term on the right-hand side both follow from the newly generated f hopping in $\mathcal{H}_{1,\lambda}$ and the special form of the anticommutator relations, Eq. (3). Note that only f electron operators acting on different sites $i \neq j$ contribute to the second term. As an approximation, we may replace the operator D_{jm} by its expectation value

$$D = \langle D_{jm} \rangle = 1 - \frac{\nu_f - 1}{\nu_f} \langle \hat{n}^f_j \rangle, \tag{31}$$

where $\langle \hat{n}^f_j \rangle = \Sigma_m \langle \hat{f}^{\dagger}_{jm} \hat{f}^{\dagger}_{jm} \rangle$ is the average f site occupation and D_{jm} was defined in Eq. (2). Note that the average D is independent of j and m. Finally, by neglecting spin-flip processes [third term in Eq. (30)], we obtain

$$\mathcal{L}_{0,\lambda} \hat{f}^{\dagger}_{\mathbf{k}m} c_{\mathbf{k}m} = [\varepsilon_{f,\lambda} + D(\gamma_{\mathbf{k},\lambda} - \bar{\gamma}_\lambda) - \varepsilon_{\mathbf{k},\lambda}] \hat{f}^{\dagger}_{\mathbf{k}m} c_{\mathbf{k}m},$$

where $\bar{\gamma}_\lambda = (1/N) \Sigma_{\mathbf{k}} \gamma_{\mathbf{k},\lambda}$ is the averaged f dispersion. Similarly, we can evaluate the excitation energies caused by the Coulomb repulsion. We find

$$\mathcal{L}_{0,\lambda} a_{\mathbf{k},\mathbf{k}+\mathbf{q},m} = (\varepsilon_{\mathbf{k},\lambda} - \varepsilon_{\mathbf{k}+\mathbf{q},\lambda}) a_{\mathbf{k},\mathbf{k}+\mathbf{q},m} + \frac{1}{N} \sum_{\mathbf{p}} (\gamma_{\mathbf{p},\lambda} - \gamma_{\mathbf{p}-\mathbf{q},\lambda}) b_{\mathbf{k},\mathbf{k}+\mathbf{q},\mathbf{p},m}, \tag{32}$$

where

$$b_{\mathbf{k},\mathbf{k}+\mathbf{q},\mathbf{p},m} = \frac{1}{N}\delta(c^{\dagger}_{\mathbf{k}m}c_{\mathbf{k}+\mathbf{q},m}) \sum_{i\neq j,m'} \delta(\hat{f}^{\dagger}_{im'}\hat{f}_{jm'})e^{i\mathbf{q}\mathbf{R}_j}e^{i\mathbf{p}(\mathbf{R}_i-\mathbf{R}_j)}. \tag{33}$$

Due to the fluctuation operators in $a_{\mathbf{k},\mathbf{k}+\mathbf{q},\lambda}$ no additional term appears in Eq. (32). For a weak hybridization V, the effective dispersion energy of the f electrons, $\gamma_{\mathbf{k},\lambda} \sim V^2/(\varepsilon_{\mathbf{k}}-\varepsilon_f)$, is small and the last term in Eq. (32) can be neglected. Thus we can write

$$\mathcal{H}_{1,\lambda} = \mathbf{P}_\lambda \mathcal{H}_1 = \sum_{\mathbf{k},m} \Theta(\lambda - |\varepsilon_{f,\lambda} + D(\gamma_{\mathbf{k},\lambda} - \bar{\gamma}_\lambda) - \varepsilon_{\mathbf{k},\lambda}|) \times V_{\mathbf{k},\lambda}(\hat{f}^{\dagger}_{\mathbf{k}m}c_{\mathbf{k}m} + \text{H.c.}) + \sum_{\mathbf{k},\mathbf{q},m} \Theta(\lambda - |\varepsilon_{\mathbf{k},\lambda} - \varepsilon_{\mathbf{k}+\mathbf{q},\lambda}|)U_{\mathbf{k},\mathbf{k}+\mathbf{q},\lambda}a_{\mathbf{k},\mathbf{k}+\mathbf{q},m},$$

where the Θ functions ensure that $\mathbf{Q}_\lambda \mathcal{H}_\lambda = 0$ is fulfilled. With this expression for $\mathcal{H}_{1,\lambda}$, the generator $X_{\lambda,\Delta\lambda}$ can be written in close analogy to Eq. (21) as

$$X_{\lambda,\Delta\lambda} = \sum_{\mathbf{k},m} \alpha_{\mathbf{k}}(\lambda,\Delta\lambda)(\hat{f}^{\dagger}_{\mathbf{k}m}c_{\mathbf{k}m} - \text{H.c.}) + \sum_{\mathbf{k}\mathbf{q},m} \beta_{\mathbf{k},\mathbf{k}+\mathbf{q}}(\lambda,\Delta\lambda)a_{\mathbf{k},\mathbf{k}+\mathbf{q},m}, \tag{34}$$

with parameters $\alpha_{\mathbf{k}}(\lambda,\Delta\lambda)$ and $\beta_{\mathbf{k},\mathbf{k}+\mathbf{q}}(\lambda,\Delta\lambda)$ that have to be chosen in such a way that the condition $\mathbf{Q}_{\lambda-\Delta\lambda}\mathcal{H}_{\lambda-\Delta\lambda}=0$ is satisfied. Using the abbreviations

$$A_{\mathbf{k},\lambda} = \varepsilon_{f,\lambda} + D(\gamma_{\mathbf{k},\lambda} - \bar{\gamma}_\lambda) - \varepsilon_{\mathbf{k},\lambda},$$

$$B_{\mathbf{k},\mathbf{k}+\mathbf{q},\lambda} = \varepsilon_{\mathbf{k},\lambda} - \varepsilon_{\mathbf{k}+\mathbf{q},\lambda}, \tag{35}$$

we make the ansatz

$$\alpha_{\mathbf{k}}(\lambda,\Delta\lambda) = \Delta\lambda \frac{A_{\mathbf{k},\lambda}\Theta(\lambda - |A_{\mathbf{k},\lambda}|)}{\kappa(\lambda - |A_{\mathbf{k},\lambda}|)^2} V_{\mathbf{k},\lambda},$$

$$\beta_{\mathbf{k},\mathbf{k}+\mathbf{q}}(\lambda,\Delta\lambda) = \Delta\lambda \frac{B_{\mathbf{k},\mathbf{k}+\mathbf{q},\lambda}\Theta(\lambda - |B_{\mathbf{k},\mathbf{k}+\mathbf{q},\lambda}|)}{\kappa(\lambda - |B_{\mathbf{k},\mathbf{k}+\mathbf{q},\lambda}|)^2} U_{\mathbf{k},\mathbf{k}+\mathbf{q},\lambda}. \tag{36}$$

We will show that this is an appropriate choice for the continuous formulation of the PRM. The constant κ denotes an energy constant to ensure that the parameters $\alpha_{\mathbf{k}}(\lambda,\Delta\lambda)$ and $\beta_{\mathbf{k},\mathbf{k}+\mathbf{q}}(\lambda,\Delta\lambda)$ are dimensionless.

B. Renormalization equations

In order to derive renormalization equations for the parameters of Hamiltonian (23), we compare two alternative expressions for $\mathcal{H}_{\lambda-\Delta\lambda}$ that allow to find relations between the parameters at cutoffs λ and $\lambda-\Delta\lambda$. The first expression for $\mathcal{H}_{\lambda-\Delta\lambda}$ is obtained by writing the renormalization ansatz, Eq. (22), for the reduced cutoff $\lambda-\Delta\lambda$ instead of λ,

$$\mathcal{H}_{\lambda-\Delta\lambda} := \mathcal{H}_\lambda|_{\lambda\to\lambda-\Delta\lambda}. \tag{37}$$

The second expression follows from the direct evaluation of the unitary transformation, Eq. (13). Since both $\alpha_{\mathbf{k}}(\lambda,\Delta\lambda)$ and $\beta_{\mathbf{k},\mathbf{k}+\mathbf{p}}(\lambda,\Delta\lambda)$ are proportional to $\Delta\lambda$, this yields

$$\mathcal{H}_{\lambda-\Delta\lambda} = e^{X_{\lambda,\Delta\lambda}}\mathcal{H}_\lambda e^{-X_{\lambda,\Delta\lambda}} \approx \mathcal{H}_\lambda + [X_{\lambda,\Delta\lambda},\mathcal{H}_\lambda]. \tag{38}$$

Comparing the operators in Eq. (37) with the equivalent operators from Eq. (38), which are obtained after an additional factorization of the commutator expression, one finds difference equations for the λ-dependent parameters of $\mathcal{H}_\lambda$. The final renormalization equations in differential form are obtained in the limit $\Delta\lambda\to 0$,

$$\frac{d\varepsilon_{\mathbf{k},\lambda}}{d\lambda} = 2DV_{\mathbf{k},\lambda}\tilde{\alpha}_{\mathbf{k},\lambda} + \frac{2}{N}\sum_{\mathbf{q}} C^{ff}_{\rho}(\mathbf{q})U_{\mathbf{k},\mathbf{k}+\mathbf{q},\lambda}\tilde{\beta}_{\mathbf{k}+\mathbf{q},\mathbf{k},\lambda},$$

$$\frac{d\varepsilon_{f,\lambda}}{d\lambda} = -\frac{(\nu_f-1)}{N}\sum_{\mathbf{k}}(\gamma_{\mathbf{k},\lambda}-\bar{\gamma}_\lambda)\tilde{\alpha}_{\mathbf{k},\lambda}\langle\hat{f}^{\dagger}_{\mathbf{k}m}c_{\mathbf{k}m} + \text{H.c.}\rangle - \frac{2}{N}\sum_{\mathbf{k}} V_{\mathbf{k},\lambda}\tilde{\alpha}_{\mathbf{k},\lambda}[1+(\nu_f-1)\langle c^{\dagger}_{\mathbf{k}m}c_{\mathbf{k}m}\rangle] - \frac{2-4\langle n^f\rangle}{N^2}\sum_{\mathbf{k},\mathbf{q},m'} U_{\mathbf{k},\mathbf{k}+\mathbf{q},\lambda}\tilde{\beta}_{\mathbf{k}+\mathbf{q},\mathbf{k},\lambda}\langle c^{\dagger}_{\mathbf{k}+\mathbf{q},m'}c_{\mathbf{k}+\mathbf{q},m'}\rangle,$$

$$\frac{d\gamma_{\mathbf{k},\lambda}}{d\lambda} = -2V_{\mathbf{k},\lambda}\tilde{\alpha}_{\mathbf{k},\lambda},$$

$$\frac{dg_{\mathbf{k},\lambda}}{d\lambda} = -\frac{1}{N}\sum_{\mathbf{q},m} U_{\mathbf{q},\mathbf{q}+\mathbf{k},\lambda}\tilde{\beta}_{\mathbf{q}+\mathbf{k},\mathbf{q},\lambda}(\langle c^{\dagger}_{\mathbf{q}+\mathbf{k},m}c_{\mathbf{q}+\mathbf{k},m}\rangle - \langle c^{\dagger}_{\mathbf{q}m}c_{\mathbf{q}m}\rangle) - \frac{1}{N^2}\sum_{\mathbf{q},\mathbf{k}',m} U_{\mathbf{q},\mathbf{q}+\mathbf{k}',\lambda}\tilde{\beta}_{\mathbf{q}+\mathbf{k}',\mathbf{q},\lambda}(\langle c^{\dagger}_{\mathbf{q}+\mathbf{k}',m}c_{\mathbf{q}+\mathbf{k}',m}\rangle - \langle c^{\dagger}_{\mathbf{q}m}c_{\mathbf{q}m}\rangle),$$

$$\frac{dV_{\mathbf{k},\lambda}}{d\lambda} = A_{\mathbf{k},\lambda}\tilde{\alpha}_{\mathbf{k},\lambda},$$

$$\frac{dU_{\mathbf{k},\mathbf{k}+\mathbf{q},\lambda}}{d\lambda} = B_{\mathbf{k},\mathbf{k}+\mathbf{q},\lambda}\tilde{\beta}_{\mathbf{k},\mathbf{k}+\mathbf{q},\lambda}. \tag{39}$$

Here, we have introduced

$$\tilde{\alpha}_{\mathbf{k},\lambda} = \lim_{\Delta\lambda\to 0}\frac{\alpha_{\mathbf{k}}(\lambda,\Delta\lambda)}{\Delta\lambda},$$

$$\tilde{\beta}_{\mathbf{k},\mathbf{k}+\mathbf{q},\lambda} = \lim_{\Delta\lambda\to 0}\frac{\beta_{\mathbf{k},\mathbf{k}+\mathbf{q}}(\lambda,\Delta\lambda)}{\Delta\lambda}. \tag{40}$$

In principle, also an equation for the energy shift E_λ can be derived. Note that the renormalization Eq. (39) depend on expectation values, which enter due to a factorization approximation as discussed in the last section. Here,

$$C^{ff}_{\rho}(\mathbf{q}) = \frac{1}{N}\sum_{\substack{i,j\\ m,m'}}\langle\delta\hat{n}^f_{im}\delta\hat{n}^f_{jm'}\rangle e^{i\mathbf{q}(\mathbf{R}_i-\mathbf{R}_j)} \tag{41}$$

is a wave-vector-dependent density-density correlation function for the f electrons. This quantity as well as the other

expectation values $\langle c^{\dagger}_{\mathbf{k}m}c_{\mathbf{k}m}\rangle$, $\langle \hat{f}^{\dagger}_{\mathbf{k}m}c_{\mathbf{k}m}+\text{H.c.}\rangle$, $\langle \hat{n}^f\rangle$, and D in Eq. (39) have to be determined self-consistently within the renormalization procedure.

The renormalization equations will be evaluated by integrating Eq. (39) between the cutoff $\lambda=\Lambda$ of the original Hamiltonian and $\lambda=0$. Thereby, all transitions caused by the hybridization and the Coulomb repulsion will be eliminated. This leads to the renormalized Hamiltonian

$$\tilde{\mathcal{H}} = \sum_{\mathbf{k},m} \tilde{\varepsilon}_{\mathbf{k}} c^{\dagger}_{\mathbf{k}m} c_{\mathbf{k}m} + \tilde{\epsilon}^f \sum_{i,m} \hat{f}^{\dagger}_{im}\hat{f}_{im} + \tilde{E} + \sum_{\substack{i\neq j\\ m,m'}} \tilde{g}_{ij}\delta\hat{n}^f_{im}\delta\hat{n}^f_{jm'} + \sum_{\mathbf{k},m} \tilde{\gamma}_{\mathbf{k}}(\hat{f}^{\dagger}_{\mathbf{k}m}\hat{f}_{\mathbf{k}m})_{\text{NL}}. \tag{42}$$

Here $\tilde{\epsilon}^f=\tilde{\varepsilon}_f-\tilde{\bar{\gamma}}_\lambda$ is denoted for a renormalized f level. In the final result (42) the operator part $\mathcal{H}_{1,\lambda}$ has completely disappeared, i.e., $\mathcal{H}_{1,\lambda=0}=0$.

Note that from the commutator $[X_{\lambda,\Delta\lambda},\mathcal{H}_\lambda]$ some "higher-order" terms have been neglected, which are not present in $\mathcal{H}_\lambda$. In particular, the remaining fluctuation operators beyond the factorization approximation have been left out. *A priori* it is not clear whether or not the *neglected* terms are relevant for the physical behavior of the model. To investigate this question, one would have to add contributions to the Hamiltonian of the same operator type and to write down renormalization equations for the new set of parameters. For example, a contribution in $[X_{\lambda,\Delta\lambda},\mathcal{H}_\lambda]$ that has been neglected has the form

$$\sim \frac{1}{\sqrt{N}}\sum_{\mathbf{k}\mathbf{k}'}\sum_{\alpha\beta}\Theta(\lambda-|\varepsilon_{\mathbf{k},\lambda}-\varepsilon_{\mathbf{k}',\lambda}|)\tilde{\alpha}_{\mathbf{k},\lambda}V_{\mathbf{k}',\lambda}\times \mathbf{S}_{\mathbf{k}-\mathbf{k}'}\sigma_{\alpha\beta}c^{\dagger}_{\mathbf{k}'\alpha}c_{\mathbf{k}\beta} \tag{43}$$

(where $\sigma_{\alpha\beta}$ are Pauli matrices). It arises from the anticommutator relation (3), when spin-flip processes are included. Obviously, the term, Eq. (43), resembles the Kondo exchange, which is known from transforming the PAM to the Kondo Hamiltonian by use of the Schrieffer-Wolff transformation. The Kondo exchange becomes important in the Kondo regime of the PAM, when $\langle n^f\rangle=1$, but is of minor importance in the intermediate valence regime. All new renormalization contributions should either vanish for $\lambda\to 0$ or should at least not change significantly the behavior of the original parameters. In that respect, the present approach completely resembles the flow equation approach of Wegner.[36]

C. Renormalization of $\tilde{\mathcal{H}}$

In the Hamiltonian $\tilde{\mathcal{H}}$, conduction electrons and f electrons are decoupled, $\tilde{\mathcal{H}}=\tilde{\mathcal{H}}^c+\tilde{\mathcal{H}}^f$. However, the f part cannot be solved due to the presence of the hopping term $\tilde{\gamma}_{\mathbf{k}}$ and the interaction term $\tilde{g}_{ij}$. Thus, in order to evaluate the average density $\langle\hat{n}^f\rangle$ and the density-density correlation function $C^{ff}_\rho(\mathbf{q})$, we have to apply the PRM a second time. Here the aim is to eliminate the $\tilde{\gamma}_{\mathbf{k}}$ term of $\tilde{\mathcal{H}}^f$. Since U_{fc} is assumed to be larger than V, $\tilde{\gamma}_{\mathbf{k}}$ should be small compared to $\tilde{g}_{ij}$. Thus, for cutoff λ, the f electron Hamiltonian $\tilde{\mathcal{H}}^f$ can be decomposed into

$$\tilde{\mathcal{H}}^f_\lambda = \tilde{\mathcal{H}}^f_{0,\lambda} + \tilde{\mathcal{H}}^f_{1,\lambda} \tag{44}$$

with

$$\tilde{\mathcal{H}}^f_{0,\lambda} = \tilde{\epsilon}^f_\lambda \sum_{i,m}\hat{f}^{\dagger}_{im}\hat{f}_{im} + \sum_{i\neq j,m,m'}\tilde{g}_{ij,\lambda}\delta\hat{n}^f_{im}\delta\hat{n}^f_{jm'} + \tilde{E}_\lambda,$$

$$\tilde{\mathcal{H}}^f_{1,\lambda} = \sum_{i\neq j,m}\tilde{\gamma}_{ij,\lambda}\hat{f}^{\dagger}_{im}\hat{f}_{jm}. \tag{45}$$

Here we have written the hopping term in the local space,

$$\tilde{\gamma}_{ij,\lambda} = \frac{1}{N}\sum_{\mathbf{k}}\tilde{\gamma}_{\mathbf{k},\lambda}e^{-i\mathbf{k}(\mathbf{R}_i-\mathbf{R}_j)}. \tag{46}$$

The initial conditions for the second PRM are, according to Eq. (42),

$$\tilde{\epsilon}^f_\Lambda=\tilde{\epsilon}^f,\quad \tilde{g}_{ij,\Lambda}=\tilde{g}_{ij},\quad \tilde{\gamma}_{ij,\Lambda}=\tilde{\gamma}_{ij},\quad \tilde{E}_\Lambda=\tilde{E}. \tag{47}$$

In order to derive renormalization equations for the parameters of Hamiltonian (44), we again apply a unitary transformation from λ to $\lambda-\Delta\lambda$ on $\tilde{\mathcal{H}}^f_\lambda$,

$$\tilde{\mathcal{H}}^f_{\lambda-\Delta\lambda} = e^{X^f_{\lambda,\Delta\lambda}}\tilde{\mathcal{H}}^f_\lambda e^{-X^f_{\lambda,\Delta\lambda}}. \tag{48}$$

Similar to the renormalization before, an ansatz for the generator $X^f_{\lambda,\Delta\lambda}$ can be found from lowest-order perturbation theory

$$X^f_{\lambda,\Delta\lambda} = \sum_{\substack{i,j\neq i\\ m}}\alpha^f_{ij}(\lambda,\Delta\lambda)\mathcal{A}^f_{m,ij}. \tag{49}$$

Here

$$\mathcal{A}^f_{m,ij} = \frac{2}{\omega_{ij,\lambda}}\left(\sum_{\substack{i,r\neq i\\ n}}\tilde{g}_{ri,\lambda}\delta\hat{n}^f_{rn}\hat{f}^{\dagger}_{im}\hat{f}_{jm} - \sum_{\substack{i,r\neq j\\ n}}\tilde{g}_{rj,\lambda}\hat{f}^{\dagger}_{im}\hat{f}_{jm}\delta\hat{n}^f_{rn}\right)$$

with the prefactor

$$\alpha^f_{ij}(\lambda,\Delta\lambda) = \frac{\omega_{ij,\lambda}\gamma_{ij,\lambda}\Theta(\lambda-|\omega_{ij,\lambda}|)}{\kappa(\lambda-|\omega_{ij,\lambda}|)^2}\Delta\lambda, \tag{50}$$

where

$$\omega_{ij,\lambda} = \pm 2\left[\sum_{\substack{r,s\neq\{i,j\}\\ nn'}}(\tilde{g}_{ri,\lambda}\tilde{g}_{si,\lambda}-2\tilde{g}_{ri,\lambda}\tilde{g}_{sj,\lambda} + \tilde{g}_{rj,\lambda}\tilde{g}_{sj,\lambda})\langle\delta\hat{n}^f_{rn}\delta\hat{n}^f_{sn'}\rangle\right]^{1/2}.$$

The renormalization equations for the parameters of the Hamiltonian are found by comparing the expression (44) for $\tilde{\mathcal{H}}^f_\lambda$, where λ is replaced by $\lambda-\Delta\lambda$, with the expression for $\tilde{\mathcal{H}}^f_{\lambda-\Delta\lambda}$, which is obtained by direct evaluation of the unitary transformation, Eq. (48). One finds

$$\frac{d\tilde{\epsilon}^f_\lambda}{d\lambda} = -\frac{2D}{N^3}\sum_{\{j,l,r\}\neq i,m}\Bigg[\tilde{\gamma}_{lj,\lambda}(\tilde{g}_{ir,\lambda}-\tilde{g}_{il,\lambda})\frac{\tilde{\alpha}^f_{rl,\lambda}}{\omega_{rl,\lambda}} - \tilde{\gamma}_{rl,\lambda}(\tilde{g}_{il,\lambda} - \tilde{g}_{ij,\lambda})\frac{\tilde{\alpha}^f_{lj,\lambda}}{\omega_{lj,\lambda}}\Bigg]\langle \hat{f}^\dagger_{rm}\hat{f}_{jm}\rangle,$$

$$\frac{d\tilde{g}_{ij,\lambda}}{d\lambda} = -\frac{4}{N^2}\sum_{\substack{r,s\neq r\\ m}}(\tilde{g}_{sj,\lambda}-\tilde{g}_{rj,\lambda})(\tilde{g}_{ir,\lambda}-\tilde{g}_{is,\lambda})\frac{\tilde{\alpha}^f_{rs,\lambda}}{\omega_{rs,\lambda}}\langle \hat{f}^\dagger_{rm}\hat{f}_{sm}\rangle,$$

$$\frac{d\tilde{\gamma}_{ij,\lambda}}{d\lambda} = \omega_{ij,\lambda}\tilde{\alpha}^f_{ij,\lambda}, \tag{51}$$

where

$$\tilde{\alpha}^f_{ij,\lambda} = \lim_{\Delta\lambda\to 0}\frac{\alpha^f_{ij}(\lambda,\Delta\lambda)}{\Delta\lambda}. \tag{52}$$

Solving the set of differential Eq. (51) with the initial conditions, Eq. (47), one finds the renormalized parameters for $\lambda\to 0$. Thus, the fully renormalized Hamiltonian for the f electron part reads

$$\tilde{\tilde{\mathcal{H}}}^f = \tilde{\tilde{\epsilon}}^f\sum_{i,m}\hat{n}^f_{im} + \sum_{i\neq j,m,m'}\tilde{\tilde{g}}_{ij}\delta\hat{n}^f_{im}\delta\hat{n}^f_{jm'} + \tilde{\tilde{E}}, \tag{53}$$

where the double tildes denote the parameter values for $\lambda\to 0$. Note that the effective Hamiltonian $\tilde{\tilde{\mathcal{H}}}^f$ describes a lattice-gas model of ions, which interact via a possibly long-range interaction $\tilde{\tilde{g}}_{ij}$. Since all local-density operators commute, we can use either classical Monte Carlo simulations or an exact-diagonalization (ED) approach to evaluate the expectation values $\langle\hat{n}^f\rangle_{\tilde{\tilde{\mathcal{H}}}^f}$ and $C^{ff}_{\rho,ij}\approx\Sigma_{mm'}\langle\delta\hat{n}^f_{im}\delta\hat{n}^f_{jm'}\rangle_{\tilde{\tilde{\mathcal{H}}}^f}$ which are formed with $\tilde{\tilde{\mathcal{H}}}^f$.

Together with the conduction electron part of Eq. (42), the final Hamiltonian reads

$$\tilde{\tilde{\mathcal{H}}} = \sum_{\mathbf{k},m}\tilde{\varepsilon}_{\mathbf{k}}c^\dagger_{\mathbf{k}m}c_{\mathbf{k}m} + \tilde{\tilde{\epsilon}}^f\sum_{i,m}\hat{f}^\dagger_{im}\hat{f}_{im} + \sum_{i\neq j,m,m'}\tilde{\tilde{g}}_{ij}\delta\hat{n}^f_{im}\delta\hat{n}^f_{im'} + \tilde{\tilde{E}}. \tag{54}$$

Note that this result resembles the effective Hamiltonian of the PRM applied to the Falicov-Kimball model.[26]

D. Expectation values

Finally, we have to evaluate the expectation values in the renormalization equations. According to Sec. IV B they are formed with the full Hamiltonian $\mathcal{H}$. Let us start from relation (17) which states that both the Hamiltonian and the operators in expectation values are subject to the same unitary transformation. As an example, let us consider $\langle c^\dagger_{\mathbf{k}m}c_{\mathbf{k}m}\rangle$. One way to evaluate this quantity would be to derive renormalization equations for the composite operator $(c^\dagger_{\mathbf{k}m}c_{\mathbf{k}m})_\lambda$. The resulting equation looks similar to Eq. (37) since the Hamiltonian $\mathcal{H}_\lambda$ contains the operator product $c^\dagger_{\mathbf{k}m}c_{\mathbf{k}m}$. However, different initial parameter values at cutoff Λ would have to be taken for each value of $\mathbf{k}$. The remaining expectation values $\langle\hat{n}^f\rangle$ and $\langle\hat{f}^\dagger_{\mathbf{k}m}c_{\mathbf{k}m}+\text{H.c.}\rangle$ can be evaluated in the same way. However, in order to restrict the numerical effort, we shall proceed differently by deriving separate renormalization equations for single fermion creation or annihilation operators $\hat{f}^{(\dagger)}_{\mathbf{k}m}$ and $c^{(\dagger)}_{\mathbf{k}m}$. For instance, for $(c^\dagger_{\mathbf{k}m}c_{\mathbf{k}m})_\lambda = c^\dagger_{\mathbf{k}m,\lambda}c_{\mathbf{k}m,\lambda}$ we make the ansatz

$$c^\dagger_{\mathbf{k}m,\lambda} = x_{\mathbf{k},\lambda}c^\dagger_{\mathbf{k}m} + y_{\mathbf{k},\lambda}\hat{f}^\dagger_{\mathbf{k}m}, \tag{55}$$

where $x_{\mathbf{k},\lambda}$ and $y_{\mathbf{k},\lambda}$ are λ-dependent coefficients with the initial values

$$x_{\mathbf{k},\Lambda} = 1, \quad y_{\mathbf{k},\Lambda} = 0 \tag{56}$$

at $\lambda=\Lambda$. The operator structure of $c^\dagger_{\mathbf{k}m,\lambda}$ in Eq. (55) is derived from the first-order expression in V. Thereby, less important contributions from U_{fc} to the new generator X_λ will be neglected. This is in contrast to the influence of U_{fc} on the renormalized conduction electron dispersion $\tilde{\varepsilon}_{\mathbf{k}}$ where additional gaps appear due to the presence of the Coulomb repulsion U_{fc}.

To assure that the λ-dependent operators $c_{\mathbf{k}m,\lambda}$ and $c^\dagger_{\mathbf{k}m,\lambda}$ fulfill fermionic anticommutator relations, the identity

$$|x_{\mathbf{k},\lambda}|^2 + D|y_{\mathbf{k},\lambda}|^2 = 1 \tag{57}$$

must hold. Proceeding analogous to the renormalization procedure for $\mathcal{H}_\lambda$, we find the differential equations,

$$\frac{dx_{\mathbf{k},\lambda}}{d\lambda} = Dy_{\mathbf{k},\lambda}\tilde{\alpha}_{\mathbf{k},\lambda}, \quad \frac{dy_{\mathbf{k},\lambda}}{d\lambda} = -x_{\mathbf{k},\lambda}\tilde{\alpha}_{\mathbf{k},\lambda}. \tag{58}$$

For the transformation of $\hat{f}^\dagger_{\mathbf{k}m}$, we use the corresponding ansatz,

$$\hat{f}^\dagger_{\mathbf{k}m,\lambda} = -Dy_{\mathbf{k},\lambda}c^\dagger_{\mathbf{k}m} + x_{\mathbf{k},\lambda}\hat{f}^\dagger_{\mathbf{k}m}, \tag{59}$$

which allows to evaluate the expectation values $\langle\hat{n}^f\rangle$ and $\langle\hat{f}^\dagger_{\mathbf{k}m}c_{\mathbf{k}m}+\text{H.c.}\rangle$. Solving the differential Eq. (58) with the initial conditions, Eq. (56) and taking the limit $\lambda\to 0$, we obtain the renormalized prefactors $\tilde{x}_{\mathbf{k}}$ and $\tilde{y}_{\mathbf{k}}$. Then, the expectation values can be expressed by

$$\langle c^\dagger_{\mathbf{k}m}c_{\mathbf{k}m}\rangle = |\tilde{x}_{\mathbf{k}}|^2 f(\tilde{\varepsilon}_{\mathbf{k}}) + |\tilde{y}_{\mathbf{k}}|^2\langle\hat{f}^\dagger_{\mathbf{k}m}\hat{f}_{\mathbf{k}m}\rangle_{\tilde{\mathcal{H}}},$$

$$\langle\hat{f}^\dagger_{\mathbf{k}m}\hat{f}_{\mathbf{k}m}\rangle = D^2|\tilde{y}_{\mathbf{k}}|^2 f(\tilde{\varepsilon}_{\mathbf{k}}) + |\tilde{x}_{\mathbf{k}}|^2\langle\hat{f}^\dagger_{\mathbf{k}m}\hat{f}_{\mathbf{k}m}\rangle_{\tilde{\mathcal{H}}},$$

$$\langle\hat{f}^\dagger_{\mathbf{k}m}c_{\mathbf{k}m}+\text{H.c.}\rangle = -2\tilde{x}_{\mathbf{k}}\tilde{y}_{\mathbf{k}}[Df(\tilde{\varepsilon}_{\mathbf{k}}) - \langle\hat{f}^\dagger_{\mathbf{k}m}\hat{f}_{\mathbf{k}m}\rangle_{\tilde{\mathcal{H}}}], \tag{60}$$

where

$$f(\tilde{\varepsilon}_{\mathbf{k}}) = \langle c^\dagger_{\mathbf{k}m}c_{\mathbf{k}m}\rangle_{\tilde{\mathcal{H}}} = \frac{1}{e^{\beta\tilde{\varepsilon}_{\mathbf{k}}}+1} \tag{61}$$

is the Fermi function for the renormalized conduction electrons and $\beta=1/T$ is the inverse temperature.

To evaluate the expectation value $\langle\hat{f}^\dagger_{\mathbf{k}m}\hat{f}_{\mathbf{k}m}\rangle_{\tilde{\mathcal{H}}}$, one can apply the second renormalization transformation from Sec. IV C which was used before to renormalize $\tilde{\mathcal{H}}$. Taking $\tilde{\mathcal{H}}^f_{1,\lambda}$ from Eq. (45) as perturbation, $\langle\hat{f}^\dagger_{\mathbf{k}m}\hat{f}_{\mathbf{k}m}\rangle_{\tilde{\mathcal{H}}}$ can be expressed by new expectation values which are formed with $\tilde{\tilde{\mathcal{H}}}^f$, defined in

Eq. (58). However, it turns out that the density-density term $\sim\tilde{\tilde{g}}_{ij}$ can be neglected in the f part of $\tilde{\tilde{\mathcal{H}}}$. For a qualitative argument for this approximation let us consider the density-density correlation function of f electrons, $\langle\delta\hat{n}_i^f\delta\hat{n}_j^f\rangle_{\tilde{\tilde{\mathcal{H}}}}$ at finite temperature, which can be evaluated by classical Monte Carlo techniques. As already mentioned, $\tilde{\tilde{\mathcal{H}}}$ agrees with the effective Hamiltonian of the Falicov-Kimball model (FKM),[26] obtained by applying the PRM. For this model it was shown that $\langle\delta\hat{n}_i^f\delta\hat{n}_j^f\rangle_{\tilde{\tilde{\mathcal{H}}}}$ has a maximum at $\mathbf{R}_i=\mathbf{R}_j$ and decreases exponentially with increasing distance $|\mathbf{R}_i-\mathbf{R}_j|$. Thus, for finite temperatures we have

$$\sum_{m,m'}\langle\delta\hat{n}_{im}^f\delta\hat{n}_{jm'}^f\rangle_{\tilde{\tilde{\mathcal{H}}}}\approx\delta_{ij}\sum_{m,m'}\langle\delta\hat{n}_{im}^f\delta\hat{n}_{im'}^f\rangle_{\tilde{\tilde{\mathcal{H}}}}\approx\delta_{ij}\langle\hat{n}^f\rangle(1-\langle\hat{n}^f\rangle). \tag{62}$$

The result depends on the average occupation $\langle\hat{n}^f\rangle$ of the f electrons. If $\langle\hat{n}^f\rangle$ is either almost zero or one, the density correlations of the f electrons become small. In the intermediate valence regime, when $\tilde{\epsilon}^f$ is close to the Fermi level, we can neglect the density contributions in the case of large U_{fc}, too, because $\langle\hat{n}^f\rangle$ changes abruptly from $\langle\hat{n}_m^f\rangle\approx 1$ to $\langle\hat{n}_m^f\rangle\approx 0$. Of course, also for small U_{fc} (i.e., in the weak-coupling limit) the g term can be neglected. Thus, omitting the $\tilde{\tilde{g}}_{ij}$ term, the renormalized Hamiltonian $\tilde{\mathcal{H}}$ reduces to

$$\tilde{\mathcal{H}}=\sum_{\mathbf{k},m}\tilde{\varepsilon}_{\mathbf{k}}c_{\mathbf{k}m}^\dagger c_{\mathbf{k}m}+\tilde{\epsilon}^f\sum_{i,m}\hat{f}_{im}^\dagger\hat{f}_{im}+\sum_{\mathbf{k},m}\tilde{\gamma}_{\mathbf{k}}(\hat{f}_{\mathbf{k}m}^\dagger\hat{f}_{\mathbf{k}m})_{\mathrm{NL}}+\tilde{E}. \tag{63}$$

Note that this Hamiltonian $\tilde{\mathcal{H}}$ has the same form as the Hamiltonian obtained by the PRM applied to the periodic Anderson model.[17,18]

Using the simplified Hamiltonian (63), we are able to evaluate $\langle\hat{f}_{\mathbf{k}m}^\dagger\hat{f}_{\mathbf{k}m}\rangle_{\tilde{\mathcal{H}}}$, although due to the unusual properties of Hubbard operators, further approximations are necessary. For this reason, let us consider the case where the renormalized f level is above the Fermi energy. Then, only few f electrons are present and a mean-field treatment of the Hubbard operators is justified. According to Ref. 17, one finds $\langle\hat{f}_{\mathbf{k}m}^\dagger\hat{f}_{\mathbf{k}m}\rangle_{\tilde{\mathcal{H}}}\approx f(\tilde{\omega}_{\mathbf{k}})$. Here, $f(\tilde{\omega}_{\mathbf{k}})$ is the Fermi function at the renormalized dispersion $\tilde{\omega}_{\mathbf{k}}$ of the f electrons, where $\tilde{\omega}_{\mathbf{k}}=\tilde{\varepsilon}_f+D(\tilde{\gamma}_{\mathbf{k}}-\bar{\tilde{\gamma}})$ and $D\approx 1$ in this case. For a general f level position, the expectation value can be written as

$$\begin{aligned}\langle\hat{f}_{\mathbf{k}m}^\dagger\hat{f}_{\mathbf{k}m}\rangle_{\tilde{\mathcal{H}}}&=\frac{1}{\mathrm{Tr}\,e^{-\beta\tilde{\mathcal{H}}}}\mathrm{Tr}(\hat{f}_{\mathbf{k}m}^\dagger\hat{f}_{\mathbf{k}m}e^{-\beta\tilde{\mathcal{H}}})\\&=\frac{1}{\mathrm{Tr}\,e^{-\beta\tilde{\mathcal{H}}}}\mathrm{Tr}(e^{\beta\tilde{\mathcal{H}}}\hat{f}_{\mathbf{k}m}e^{-\beta\tilde{\mathcal{H}}}\hat{f}_{\mathbf{k}m}^\dagger e^{-\beta\tilde{\mathcal{H}}}),\end{aligned} \tag{64}$$

where we have used $e^{-\beta\tilde{\mathcal{H}}}e^{\beta\tilde{\mathcal{H}}}=1$ and the cyclic invariance of the trace, $\mathrm{Tr}(abc)=\mathrm{Tr}(bca)$. Using Eqs. (3) and (63), we find $e^{\beta\tilde{\mathcal{H}}}\hat{f}_{\mathbf{k}m}e^{-\beta\tilde{\mathcal{H}}}\approx e^{-\beta\tilde{\omega}_{\mathbf{k}}}\hat{f}_{\mathbf{k}m}$ and hence

$$\langle\hat{f}_{\mathbf{k}m}^\dagger\hat{f}_{\mathbf{k}m}\rangle_{\tilde{\mathcal{H}}}\approx\frac{e^{-\beta\tilde{\omega}_{\mathbf{k}}}\langle\{\hat{f}_{\mathbf{k}m}^\dagger,\hat{f}_{\mathbf{k}m}\}\rangle_{\tilde{\mathcal{H}}}}{1+e^{-\beta\tilde{\omega}_{\mathbf{k}}}}=Df(\tilde{\omega}_{\mathbf{k}}). \tag{65}$$

Note that from Eq. (65) and $D=1-[(\nu_f-1)/\nu_f]\langle\hat{n}^f\rangle$ an interesting relation between the f occupation $\langle\hat{n}^f\rangle$ and the f electron dispersion $\tilde{\omega}_{\mathbf{k}}$ follows:

$$D=\frac{1}{1+\dfrac{\nu_f-1}{N}\displaystyle\sum_{\mathbf{k}}f(\tilde{\omega}_{\mathbf{k}})}.$$

Using Eq. (65), we can rewrite the expectation values in Eq. (60) as

$$\begin{aligned}\langle c_{\mathbf{k}m}^\dagger c_{\mathbf{k}m}\rangle&=|\tilde{x}_{\mathbf{k}}|^2f(\tilde{\varepsilon}_{\mathbf{k}})+D|\tilde{y}_{\mathbf{k}}|^2f(\tilde{\omega}_{\mathbf{k}}),\\\langle\hat{f}_{\mathbf{k}m}^\dagger\hat{f}_{\mathbf{k}m}\rangle&=D^2|\tilde{y}_{\mathbf{k}}|^2f(\tilde{\varepsilon}_{\mathbf{k}})+D|\tilde{x}_{\mathbf{k}}|^2f(\tilde{\omega}_{\mathbf{k}}),\end{aligned} \tag{66}$$

and

$$\langle\hat{f}_{\mathbf{k}m}^\dagger c_{\mathbf{k}m}+\mathrm{H.c.}\rangle=-2D\tilde{x}_{\mathbf{k}}\tilde{y}_{\mathbf{k}}[f(\tilde{\varepsilon}_{\mathbf{k}})-f(\tilde{\omega}_{\mathbf{k}})], \tag{67}$$

where the tilde symbols again denote the renormalized parameters in the limit $\lambda\to 0$.

At this point, all physical quantities can be calculated. Their dependence on the model parameters such as temperature T, hybridization V, Coulomb repulsion U_{fc}, etc., is found by solving the renormalization equations self-consistently: (i) start from appropriate chosen initial values for the expectation values $\langle c_{\mathbf{k}m}^\dagger c_{\mathbf{k}m}\rangle$, $\langle\hat{n}^f\rangle$, $\langle\hat{f}_{\mathbf{k}m}^\dagger c_{\mathbf{k}m}+\mathrm{H.c.}\rangle$ and integrate the differential Eqs. (39) and (58) to obtain the renormalized parameters and prefactors. (ii) Calculate a new approximation for the set of expectation values. (iii) Repeat steps (i) and (ii) until convergence is reached, i.e., the difference of two consecutive sets of expectation values is smaller than some chosen limit. Using these final expectation values, one can calculate the physical quantities of interest.

V. NUMERICAL RESULTS

In this section we present numerical results obtained by solving the renormalization equations for the EPAM. To simplify the evaluation we restrict ourselves to the one-dimensional case. In a subsequent paper, the method will be extended to two dimensions in order to discuss a possible superconducting state close to the valence transition regime. In one dimension (1D) it is also advantageous that we can treat larger systems. We can also compare our results with DMRG studies in 1D.[12] We choose a fixed total electron density $n=\langle n^c\rangle+\langle\hat{n}^f\rangle=1.75$ and an angular momentum degeneracy $\nu_f=2$. The conduction electron dispersion for the noninteracting electron band is $\bar{\varepsilon}_k=-2t\cos k$, where $t=1$ is used as the energy unit. In the following, we discuss the dependence of the renormalized dispersion $\tilde{\varepsilon}_{\mathbf{k}}$, the f electron occupation $\langle\hat{n}^f\rangle$, and the renormalized f energy $\tilde{\epsilon}^f$ on the bare f-energy $\bar{\varepsilon}_f$ in the mixed valence regime. Note that for fixed total electron density the chemical potential depends on the bare energy $\bar{\varepsilon}_f$. As long as $\bar{\varepsilon}_f$ is far below the Fermi surface all localized states are occupied and $\langle n^c\rangle\approx 0.75$ for the

TABLE I. Typical examples of ground-state configurations for different fillings.

$\langle \hat{n}^f \rangle$	Configurations
1	11111111111111111…
2/3	1101101101101101101…
1/2	1010101010101010101…
1/3	1001001001001001001…
1/4	1000100010001000100…
1/5	1000010000100001000…
…	…
0	0000000000000000000…

present case. In contrast, for large positive $\bar{\varepsilon}_f$ the localized states are approximate empty and $\langle n^c \rangle \approx 1.75$ follows.

A. Dispersion relation

Let us start with the fully renormalized dispersion $\tilde{\varepsilon}_{\mathbf{k}}$ of the conduction electrons. As was discussed before, the renormalization Eq. (39) for Hamiltonian (42) can be solved when the expectation values are known. The final Hamiltonian $\tilde{\mathcal{H}}$ describes two separated systems of renormalized electrons. The f-electron part has the form of the renormalized FKM,[26] for which the expectation values $\langle \hat{n}^f \rangle$ and correlation function $C^{ff}_{\rho,ij}$ can be evaluated either using classical Monte Carlo or ED. In contrast to the static expectation values, the proper determination of $\tilde{\varepsilon}_{\mathbf{k}}$ requires to incorporate the density-density term $\sim \delta\hat{n}^f_i \delta\hat{n}^f_j$ from Eq. (42).

For low enough temperatures, the f-electron states in the FKM favor several almost homogeneous configurations.[26,37] This can be rigorously proven[37] for large values of the Coulomb repulsion U_{fc} and is conjectured to hold for arbitrary values.[38] For the one-dimensional case, some configurations for different fillings are listed in Table I.

As a typical case, let us consider a f electron filling of $\langle \hat{n}^f \rangle = 1/3$. There are three equivalent degenerate ground states of period 3 with corresponding arrays {100…}, {010…}, and {001…}. According to Ref. 26 one obtains

$$\langle \delta\hat{n}^f_i \delta\hat{n}^f_j \rangle = \begin{cases} 2/9 & |R_j - R_i| = 0,3,6,9,\ldots \\ -1/9 & |R_j - R_i| = 1,2,4,5,\ldots \end{cases} \tag{68}$$

for the correlation function of the local-density fluctuations, where $a=1$ is used for the lattice constant. Note that the result (68) is also valid for $\langle \hat{n}^f \rangle = 2/3$. Figure 1 shows the Fourier-transformed quantity $C^{ff}_{\rho}(k)$ as a function of the momentum k for different values of $\langle \hat{n}^f \rangle$ for the configurations of Table I. In the case $\langle \hat{n}^f \rangle = 1/2$, there are two Kronecker deltas, located at $k^* = \pm\pi$. For $\langle \hat{n}^f \rangle = 1/3$, the Kronecker deltas are present at $k^* = \pm 2\pi/3$ with smaller amplitudes. In general, for $\langle \hat{n}^f \rangle = 1/m$ (m integer), increasing m leads to smaller amplitudes of the Kronecker deltas in $C^{ff}_{\rho}(k)$. Further the results for $\langle \hat{n}^f \rangle = 1/m$ and $\langle \hat{n}^f \rangle = 1 - 1/m$ coincide.

Next, we insert the Fourier-transformed correlation functions $C^{ff}_{\rho}(k)$ from Table I into the differential Eq. (39), together with some guessed initial expectation values for $\langle \hat{n}^f \rangle$,

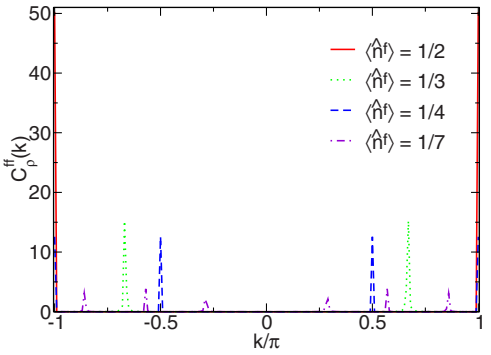

FIG. 1. (Color online) Fourier transformation $C^{ff}_{\rho}(k)$ of $\langle \delta\hat{n}^f_i \delta\hat{n}^f_j \rangle$ for different values of f electron occupations $\langle \hat{n}^f \rangle$ according to the configurations of Table I. The number of lattice sites is $N=200$.

$\langle c^{\dagger}_{km} c_{km} \rangle$, and $\langle \hat{f}^{\dagger}_{km} c_{km} + \text{H.c.} \rangle$. With the initial condition (29), we can find from the solution the renormalized Hamiltonian (42). Since it is not diagonal, we have to proceed as discussed in Sec. IV C, in order to remove the hopping part $\tilde{\mathcal{H}}^f_1$ of Eq. (44). With the fully renormalized Hamiltonian $\tilde{\tilde{\mathcal{H}}}$ of Eq. (54), we are able to recalculate the expectation values $\langle \hat{n}^f \rangle$, $\langle c^{\dagger}_{km} c_{km} \rangle$, and $\langle \hat{f}^{\dagger}_{km} c_{km} + \text{H.c.} \rangle$ by using Eq. (60) and the renormalization Eq. (58). The new expectation values are now used to repeat the self-consistent calculation until convergency is reached. For simplicity, the correlation function $C^{ff}_{\rho}(k)$ is not renormalized. Note that we also have to adjust the chemical potential μ as well as $\bar{\varepsilon}_f$ in order to fulfill the condition $n = \langle n^c \rangle + \langle \hat{n}^f \rangle = 1.75$ for a given value of $\langle \hat{n}^f \rangle$.

To illustrate the renormalization process, Fig. 2 shows the λ dependence of the hybridization $V_{k,\lambda}$ and Coulomb repulsion $U_{k,\pi/8,\lambda}$ for the first renormalization step using an one-dimensional lattice with $N=80$ sites. In this figure, $V_{k,\lambda}$ in

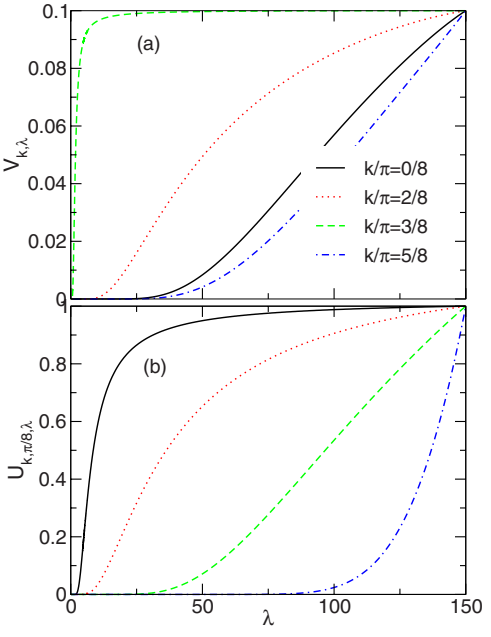

FIG. 2. (Color online) Dependence of $V_{k,\lambda}$ [panel (a)] and $U_{k,\pi/8,\lambda}$ [panel (b)] on λ for several values of momentum k at $T=0.05$, $V=0.1$, $U_{fc}=1$, and $\bar{\varepsilon}_f=-1.0$.

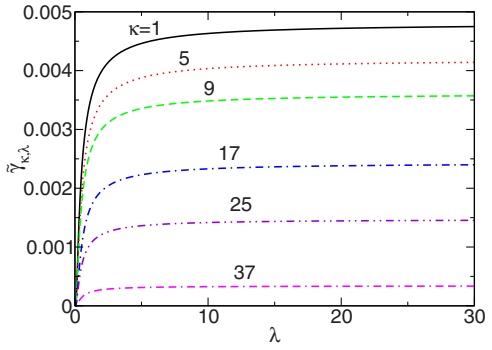

FIG. 3. (Color online) λ dependence of $\tilde{\gamma}_{\kappa,\lambda}$ for some lattice distances, $\kappa=|\mathbf{R}_i-\mathbf{R}_j|$ for $T=0.05$, $V=0.1$, $U_{fc}=1$, and $\bar{\varepsilon}_f=-1.0$.

panel (a) and $U_{k,\pi/8,\lambda}$ in panel (b), are plotted for several values of k with initial parameters $U_{fc}=1$, $V=0.1$, $\bar{\varepsilon}_f=-1$, and $T=0.05$. As expected, $V_{k,\lambda}$ and $U_{k,\pi/8,\lambda}$ decrease exponentially for all k values with decreasing λ. Hence, no contributions of the hybridization or the Coulomb interaction remain for $\lambda\to 0$. In Fig. 3, the hopping term $\tilde{\gamma}_{ij,\lambda}$ between localized electrons from Eq. (46) is shown as a function of λ for the second renormalization step and some distances $\kappa=|\mathbf{R}_i-\mathbf{R}_i|$ between lattice sites $\mathbf{R}_i$ and $\mathbf{R}_j$. As before, $\tilde{\gamma}_{ij,\lambda}$ decreases exponentially to zero, when λ approaches the excitation energies. This observation is valid for all distances κ.

Next we discuss the effective dispersions. Figure 4 shows the renormalized conduction electron energies $\tilde{\varepsilon}_k$ (black circles) as functions of k for different values of $\langle\hat{n}^f\rangle$. Due to $\varepsilon_k=\varepsilon_{-k}$, we can restrict ourselves to the positive half plane of the momentum space, $k>0$. In the case of $\langle\hat{n}^f\rangle=1/2$ [Fig. 4(a)], two gaps are present. For smaller values $\langle\hat{n}^f\rangle=1/3,1/4,1/7$, the number of gaps increases, as can be seen in panels (b)–(d). Note that one of the gaps is always caused by the hybridization V. It opens at the Fermi momentum k_F and results from the crossing of the one-particle energies of the conduction electrons and of the localized electrons in the valence transition regime. The other gaps are caused by the U_{fc} term. Here, the number of the gaps depends on the number of Kronecker deltas in the f density correlation function

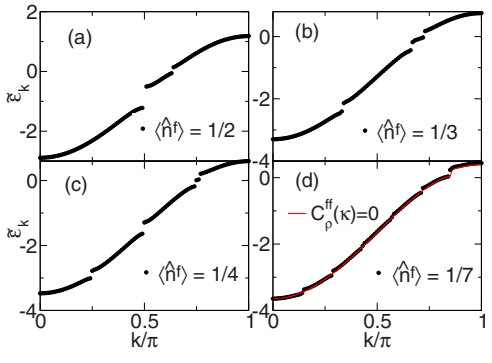

FIG. 4. (Color online) Renormalized quasiparticle energy $\tilde{\varepsilon}_k$ for several values of the localized electron density $\langle\hat{n}^f\rangle$ with $U_{fc}=1$, $V=0.1$, $T=0.05$, and $N=200$. Note that for all densities $\langle\hat{n}^f\rangle$ always one hybridization gap opens at the Fermi momentum k_F. For instance, for $\langle\hat{n}^f\rangle=1/2$ [panel (a)] $k_F\approx 0.7$. The other gaps are caused by the U_{fc} term and occur at wave vectors $k=\pi\langle\hat{n}^f\rangle l$ (l integer).

$C_\rho^{ff}(k)$ (Fig. 1). Note that $C_\rho^{ff}(q)$ enters the renormalization of $\tilde{\varepsilon}_{k,\lambda}$, Eq. (39), via a sum over q in the renormalization part due to U_{fc}. For instance, for $\langle\hat{n}^f\rangle=1/3$, there is one Kronecker delta function for $q>0$ present in $C_\rho^{ff}(q)$ at $k^*=2\pi/3$. Therefore, the main contribution in the U_{fc} part of the renormalization equation for $\varepsilon_{k,\lambda}$ occurs for k close to $k^*/2$ and $\pi-k^*/2$. Moreover, when k passes through $k^*/2$ or $\pi-k^*/2$, the sign of $\varepsilon_{k,\lambda}-\varepsilon_{k-q,\lambda}$ in $\beta_{k+q,k,\lambda}$ changes, which leads to the opening of a gap at these points. Thus, the renormalized conduction electrons dispersion for $\langle\hat{n}^f\rangle=1/3$ has two gaps at $k=\pi/3$ and $k=2\pi/3$, which are caused by the U_{fc} term.

For a general interpretation of this result, let us consider the case where the band gap is created by a weak periodic potential.[39] For a lattice with lattice constant a, the gap occurs at $k=K/2$, where K is a reciprocal-lattice vector, $K=2n\pi/a$ (n integer). For $\langle\hat{n}^f\rangle=1/3$, the f electrons in the ground state arrange with a periodicity of $3a$. Therefore, the system should behave as if it would have an effective periodicity of $3a$ or effective reciprocal-lattice vectors $K'=2n\pi/(3a)$. Thus, gaps at $k=\pi/3$ and $k=2\pi/3$ are expected in the k interval $0<k<\pi$. Note that this interpretation can also be applied to other periodic fillings in the system.

We have found that the number of Kronecker deltas in $C_\rho^{ff}(k)$ increases with decreasing values of $\langle\hat{n}^f\rangle$. However, in parallel also the weight of the Kronecker deltas decreases, as shown in Fig. 1. According to the renormalization Eq. (39) for $\varepsilon_{k,\lambda}$, this leads to a decrease in the size of the gaps caused by U_{fc}. For example, for the case $\langle\hat{n}^f\rangle=1/7$ shown in Fig. 4(d), the renormalized dispersion $\tilde{\varepsilon}_k$ has six small gaps. Comparing with $\tilde{\varepsilon}_k$ in the case of vanishing U_{fc} [the red solid line in Fig. 4(d)], yields that the energies are almost identical. Thus, the density-density correlation of the localized electrons due to U_{fc} can be neglected in this case. We conclude that correlations between localized electrons are not important for $\langle\hat{n}^f\rangle\approx 0$ and also for $\langle\hat{n}^f\rangle\approx 1$ (due to the symmetry in the f filling mentioned above). As a consequence, f correlations can be neglected for a sharp valence transition, i.e., if $\langle\hat{n}^f\rangle$ changes abruptly from 1 to 0.

In order to investigate the influence of the other parameters on the gaps, the typical case $\langle\hat{n}^f\rangle=1/3$ is again considered for some small temperature $T=0.05$. Figure 5(a) shows the renormalized energy $\tilde{\varepsilon}_k$ for $U_{fc}=1$ and different values of the hybridization V. As discussed above, the gaps have two different origins. Those caused by U_{fc} are unchanged with respect to their position in k space and to their amplitudes, if V is varied. In contrast, the gap caused by the hybridization becomes larger with increasing V. The latter behavior of $\tilde{\varepsilon}_k$ agrees with that for the usual PAM.[19,32] Figure 5(b) shows $\tilde{\varepsilon}_k$ for several values of U_{fc} and fixed hybridization $V=0.1$. In contrast to Fig. 5(a), the gaps due to U_{fc} become larger with increasing Coulomb repulsion, although their positions in k space are unchanged. This result corresponds to the discussion in Ref. 26.

To discuss the influence of the temperature, $\tilde{\varepsilon}_k$ is plotted for two different temperatures, $T=0.05$ and $T=0.2$, in Fig. 6. For the larger temperature, the f electron-density correlation function decreases exponentially as a function of the distance between lattice sites.[26] As discussed before, only the on-site correlation is important in this case, i.e., $C_\rho^{ff}(k)\approx\langle\hat{n}^f\rangle(1$

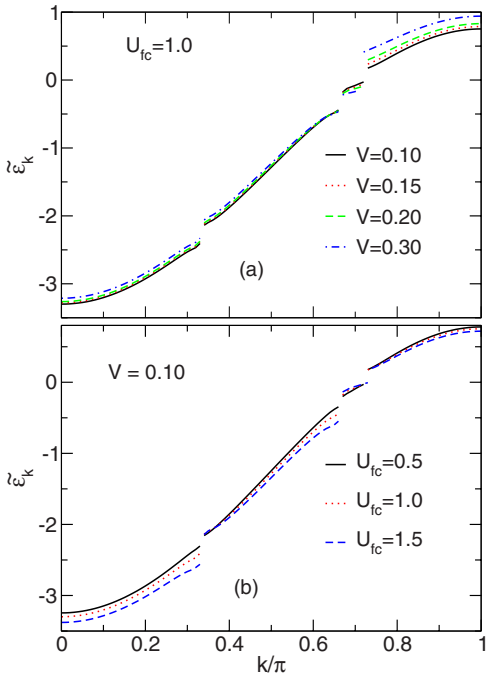

FIG. 5. (Color online) Renormalized quasiparticle energy $\tilde{\varepsilon}_k$ (a) for several values of V and $U_{fc}=1$, (b) for several values of U_{fc} and $V=0.1$ at $T=0.05$, $N=200$, and $\langle\hat{n}^f\rangle=1/3$.

$-\langle\hat{n}^f\rangle$), which does not depend on the momentum k. Therefore, the total bandwidth increases and the gaps due to the Coulomb repulsion vanish.

Note, there are no gaps in the dispersion $\tilde{\varepsilon}_k$ which are caused by U_{fc} when the "perturbation" $\mathcal{H}_1$ is put identical to zero. In that case the remaining Hamiltonian $\mathcal{H}_0$ is equivalent to the Hartree-Fock approximation. Also, in this case the dispersion $\tilde{\varepsilon}_k$ has to be solved self-consistently since the bare excitations are shifted by Hartree-Fock terms $U_{fc}\langle\hat{n}^c\rangle$ and $U_{fc}\langle\hat{n}^f\rangle$.

B. Valence transition

Next, we discuss the valence transition in some detail. Let us assume that the bare f level $\bar{\varepsilon}_f$ changes, if external pressure is applied, so that the effective f level $\tilde{\epsilon}^f$ can be shifted to the Fermi level. In this case, localized electrons can be

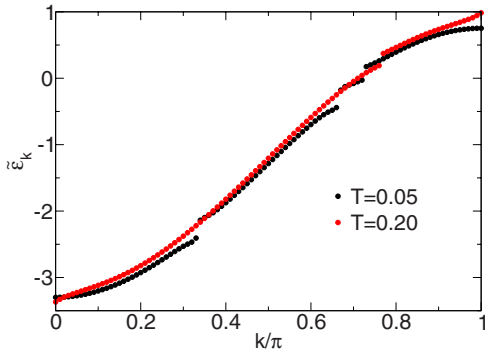

FIG. 6. (Color online) Renormalized quasiparticle energy $\tilde{\varepsilon}_k$ for two values of T and $U_{fc}=1$, $V=0.1$, $N=200$, and $\langle\hat{n}^f\rangle=1/3$.

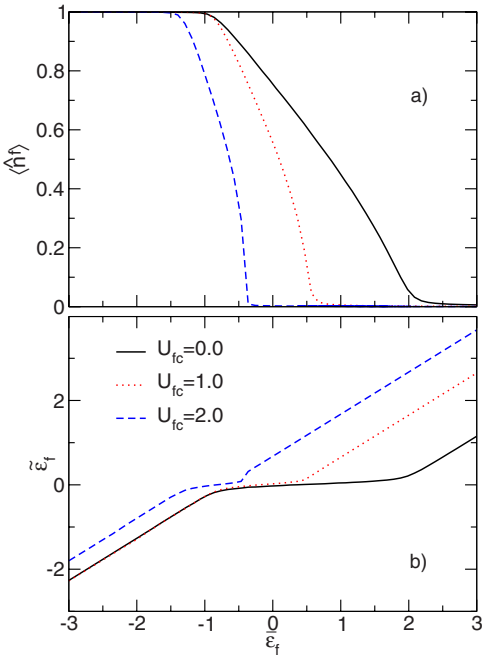

FIG. 7. (Color online) (a) Averaged f occupation number $\langle\hat{n}^f\rangle$ and (b) renormalized f level $\tilde{\epsilon}^f$ as a function of the unrenormalized f energy $\bar{\varepsilon}_f$ for several values of U_{fc} in the case of $V=0.1$ and $T=0.05$. Note that $\tilde{\epsilon}^f$ in contrast to $\bar{\varepsilon}_f$ is measured from the Fermi level.

transferred to the conduction electron band, and the f level becomes more and more depopulated, when $\tilde{\epsilon}^f$ passes the Fermi level. To discuss this phenomenon, which is called a valence transition, we consider the average f electron density $\langle\hat{n}^f\rangle$ and the renormalized f energy $\tilde{\epsilon}^f$ as functions of the bare f energy $\bar{\varepsilon}_f$. Both quantities can be evaluated from the full renormalization scheme for Hamiltonian (63). The total electron number $n=\langle\hat{n}^f\rangle+\langle n^c\rangle$ is again fixed to $n=1.75$ and a system with $N=80$ lattice sites is considered.

In Fig. 7(a), the valence transition can clearly be seen from the dependence of $\langle\hat{n}^f\rangle$ on $\bar{\varepsilon}_f$. When U_{fc} is increased the valence transition becomes sharper. At the same time, the transition regime is shifted to smaller values of $\bar{\varepsilon}_f$. The reason is that for larger U_{fc}, $\bar{\varepsilon}_f$ has to become smaller in order to satisfy the condition for the transition regime, $\bar{\varepsilon}_f+U_{fc}\langle n^c\rangle \approx \mu$. In Fig. 7(b) the corresponding curves are shown for the renormalized f electron energy $\tilde{\epsilon}^f$. Note that in the regions with $\langle\hat{n}^f\rangle\approx 1$ and $\langle\hat{n}^f\rangle\approx 0$, a linear dependence on $\bar{\varepsilon}_f$ with a slope 1 is found. Here, the renormalization contributions to $\tilde{\epsilon}^f$ are not important and $\tilde{\epsilon}^f$ is only shifted due to the chemical potential. This result completely agrees with Refs. 17 and 32 where it was assumed that for this case $\tilde{\epsilon}^f$ is determined by the mean-field contribution from U_{fc} [see Eq. (29)]. In contrast, in the mixed-valence regime, $\tilde{\epsilon}^f$ is almost independent of $\bar{\varepsilon}_f$. In this case, $\tilde{\epsilon}^f$ is fixed to the Fermi level when $\bar{\varepsilon}_f$ is varied until the f level is completely empty. Note that the width of the valence transition regime is reduced with increasing U_{fc}, which corresponds to a sharper valence transition. For $U_{fc}=2$, also a kink appears in the transition regime, which results from the sudden jump of $\langle\hat{n}^f\rangle$ in Fig. 7(a).

In the PRM, the mean-field contributions to ε_k and ε_f from the U_{fc} term are included in the initial parameter val-

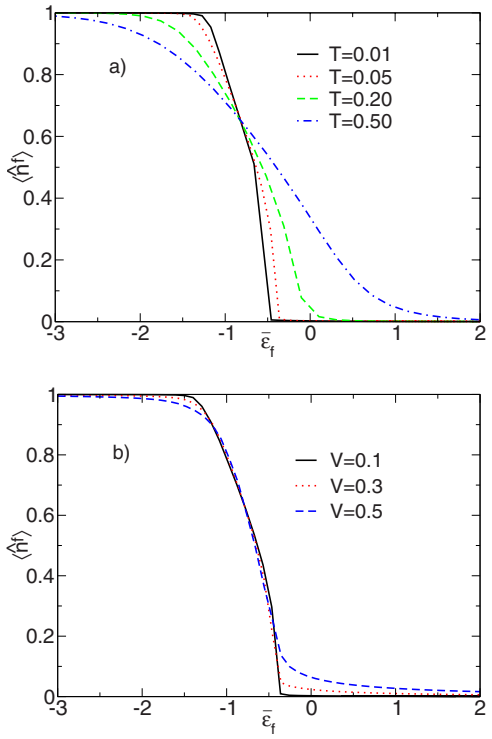

FIG. 8. (Color online) Averaged f occupation number $\langle \hat{n}^f \rangle$ as a function of the unrenormalized f energy $\bar{\varepsilon}_f$ (a) for some values of temperature T with $U_{fc}=2$, $V=0.1$ and (b) for several values of the hybridization V with $U_{fc}=2$, $T=0.05$.

ues, Eq. (29). These contributions are responsible for the shift of the valence transition to smaller values of $\bar{\varepsilon}_f$, see Fig. 7(a). If we define a valence susceptibility by $\chi_f := -\partial \langle \hat{n}^f \rangle / \partial \bar{\varepsilon}_f$, our result implies that the maximum position of χ_f is shifted to smaller values of $\bar{\varepsilon}_f$ when U_{fc} is increased. This is in contrast to slave-boson mean-field calculations,[11] where the maximum of χ_f is almost independent of U_{fc}. In order to benchmark the reliability of the PRM, we compare the present results with those obtained by DMRG calculations.[12] Unfortunately, the authors of Ref. 12 only presented properties in the valence transition regime for $U_{fc}=0$ and $U_{fc} \geq 4$. Therefore, our result can only be compared directly with the case $U_{fc}=0$. Here a detailed numerical comparison shows complete coincidence. For example, at $\bar{\varepsilon}_f=0.2$, both calculation methods give the same value $\langle \hat{n}^f \rangle = 0.69$. For the extended model with finite U_{fc}, the overall features of the results from both methods are the same. However, the DMRG calculations show a jump of the local f density $\langle \hat{n}^f \rangle$ as a function of $\bar{\varepsilon}_f$ if $U_{fc} > 5.9$. Unfortunately, the PRM is limited to not to large values of the perturbation $\mathcal{H}_1$ due to construction. In the case of the EPAM, we believe that the PRM gives reliable results in the range up to $U_{fc} \leq 5$, where no jump in $\langle \hat{n}^f \rangle$ was found. Note that in the slave-boson mean-field calculation, the jump appears for U_{fc} close to 1 (cf. Fig. 2 from Ref. 12).

To study how the valence transition depends on the temperature and on the hybridization strength, the evaluated f occupation $\langle \hat{n}^f \rangle$ is shown in Fig. 8 as a function of $\bar{\varepsilon}_f$ for different values of T and V. First, as shown in Fig. 8(a), one finds that the transition becomes sharper when the temperature T is lowered. At low temperatures, all $4f^1$ states below the Fermi energy are occupied. When the temperature is increased, also higher f states become excited leading to a $4f^0+[5d6s]$ configuration and the transition regime becomes broader. Note that in Fig. 8(a) the lowest temperature is $T=0.01$ (in units of t) for the case $U_{fc}=2$. This is not a small quantity as compared, for instance, with the superconducting transition temperature in $CeCu_2Si_2$. However, since the transition becomes sharper with decreasing temperature, the convergence of the renormalization equations is limited to temperatures above $T=0.01$.

The valence transition shows a similar behavior when the hybridization energy V is varied for fixed temperature T and fixed Coulomb repulsion U_{fc}. In Fig. 8(b), $\langle \hat{n}^f \rangle$ is shown for several values of V and $T=0.05$, $U_{fc}=2$. The valence transition becomes sharper when the hybridization becomes smaller. The transition becomes smoother when the hybridization is enhanced. Then the localized electrons easily convert into conduction electrons, and the two configurations of Ce ions, $4f^1(Ce^{3+})$ and $4f^0(Ce^{4+})$, have the tendency to become degenerate.

VI. CONCLUSIONS

In this paper, the PRM was applied to the EPAM in one dimension. In comparison to the usual periodic Anderson model, in the EPAM a local Coulomb repulsion U_{fc} between the conduction electron and the localized electron densities is included. For simplicity, also an infinite on-site Coulomb repulsion between the f electrons was assumed. As compared to previous approaches using the PRM, a more appropriate choice for the generator $X_{\lambda,\Delta\lambda}$ of the unitary transformation is used. As a consequence, the usual difference form of the renormalization equations could be replaced by differential equations which can easily be solved using existing computer subroutines. This procedure also helps to avoid some complications of previous works. On the basis of our analytical approach, a transparent physical picture for the quasiparticle dispersions and the behavior at the valence transition emerged. In particular, the gaps in the dispersion relation $\tilde{\varepsilon}_{\mathbf{k}}$ of the conduction electrons can be traced back to the presence of the hybridization V and the Coulomb repulsion U_{fc}. The total number of gaps in $\tilde{\varepsilon}_{\mathbf{k}}$ depends on the density of the localized electrons. For vanishing as well as for almost integral f occupation $\langle \hat{n}^f \rangle$, $\tilde{\varepsilon}_{\mathbf{k}}$ is not changed by the presence of U_{fc}. The valence transition is discussed as a function of various model parameters such as Coulomb repulsion U_{fc}, hybridization V, and temperature T. For fixed total electron number, we find that the valence transition becomes sharper with increasing U_{fc} and decreasing T and V. Based on the present results, in a forthcoming paper we want to extend our work to discuss the physical properties of a superconducting phase in two dimensions.

The main objective of the present approach was to discuss the physical properties of the extended PAM in the valence transition regime. In particular, we were interested in the influence of the Coulomb repulsion U_{fc} between f and conduction electrons since charge fluctuations due to the U_{fc} were claimed to lead to a superconducting phase in the in-

termediate valence regime. This problem will be discussed in a forthcoming paper. In the future, the present approach will also be extended to the Kondo phase in order to incorporate heavy-fermion behavior. The basic idea is as follows. As long as the bare $\bar{\varepsilon}_f$ is located far below the Fermi level the renormalized f level $\tilde{\varepsilon}_f$ is practically not changed and the f occupation $\langle n^f \rangle = 1$. Heavy-fermion behavior should result from this case, if additional spin-dependent interactions are included in the renormalization equations. These interactions resemble the Kondo exchange which is usually derived from the PAM by use of the Schrieffer-Wolff transformation.

It also may be interesting to compare the PRM method with the so-called X boson cumulant approach. This approach[40] was recently applied to the periodic Anderson model, leaving out the Coulomb repulsion U_{fc}. Applying a chain approximation for the one-particle Green's function, poles were found which can also be derived within the PRM. However, some simplifications are necessary.[18,19] One neglects the λ dependence of $\varepsilon_{f,\lambda}$ and approximates $\varepsilon_{f,\lambda} - D\tilde{\gamma}_\lambda$ by a λ-independent $\tilde{\varepsilon}_f$ instead of evaluating the full renormalization Eq. (39) for $\varepsilon_{f,\lambda}$. The remaining renormalization equations (with $U_{\mathbf{k},\mathbf{k}+\mathbf{q},\lambda}$ set equal to zero) can be solved analytically. In this way, one finds the same one-particle excitations as in the X boson approach of Ref. 40.

ACKNOWLEDGMENTS

We would like to thank A. Hübsch, D. Efremov, and, in particular, S. Sykora for fruitful discussions. This work was supported by the International Max-Planck Research School "Dynamical Processes in Atoms, Moleculars and Solids" and by the DFG through the research program SFB 463.

[1] H. Q. Yuan, F. M. Grosche, M. Deppe, C. Geibel, G. Sparn, and F. Steglich, Science **302**, 2104 (2003).
[2] A. T. Holmes, D. Jaccard, and K. Miyake, Phys. Rev. B **69**, 024508 (2004).
[3] F. Steglich, J. Aarts, C. D. Bredl, W. Lieke, D. Meschede, W. Franz, and H. Schäfer, Phys. Rev. Lett. **43**, 1892 (1979).
[4] N. D. Mathur, F. M. Grosche, S. R. Julian, I. R. Walker, D. M. Freye, R. K. W. Haselwimmer, and G. G. Lonzarich, Nature (London) **394**, 39 (1998).
[5] P. Monthoux and G. G. Lonzarich, Phys. Rev. B **66**, 224504 (2002).
[6] D. J. Scalapino, E. Loh, and J. E. Hirsch, Phys. Rev. B **34**, 8190 (1986).
[7] T. M. Rice and K. Ueda, Phys. Rev. B **34**, 6420 (1986).
[8] K. Miyake and H. Maebashi, J. Phys. Soc. Jpn. **71**, 1007 (2002).
[9] A. Onodera, S. Tsuduki, Y. Ohishi, T. Watanuki, K. Ishida, Y. Kitaoka, and Y. Onuki, Solid State Commun. **123**, 113 (2002).
[10] A. T. Holmes, Ph.D. thesis, University of Geneva, 2004.
[11] Y. Onishi and K. Miyake, J. Phys. Soc. Jpn. **69**, 3955 (2000).
[12] S. Watanabe, M. Imada, and K. Miyake, J. Phys. Soc. Jpn. **75**, 043710 (2006).
[13] Y. Saiga, T. Sugibayashia, and D. Hirashima, Physica B **403**, 808 (2008).
[14] T. Sugibayashi, Y. Saiga, and D. S. Hirashima, J. Phys. Soc. Jpn. **77**, 024716 (2008).
[15] K. W. Becker, A. Hübsch, and T. Sommer, Phys. Rev. B **66**, 235115 (2002).
[16] H. Tsunetsugu, M. Sigrist, and K. Ueda, Rev. Mod. Phys. **69**, 809 (1997).
[17] A. Hübsch and K. W. Becker, Eur. Phys. J. B **52**, 345 (2006).
[18] A. Mai, V. N. Phan, and K. W. Becker (unpublished).
[19] A. Hübsch, S. Sykora, and K. W. Becker, arXiv:0809.3360 (unpublished).
[20] K. S. Burch, S. V. Dordevic, F. P. Mena, A. B. Kuzmenko, D. van der Marel, J. L. Sarrao, J. R. Jeffries, E. D. Bauer, M. B. Maple, and D. N. Basov, Phys. Rev. B **75**, 054523 (2007).
[21] S. Danzenbächer *et al.*, Phys. Rev. B **75**, 045109 (2007).
[22] A. C. Hewson, *The Kondo Problem to Heavy Fermions* (Cambridge University Press, Cambridge, England, 1993).
[23] D. Khomskii and A. Kocharjan, Solid State Commun. **18**, 985 (1976).
[24] A. Hewson and P. Riseborough, Solid State Commun. **22**, 379 (1977).
[25] I. Singh, A. K. Ahuja, and S. K. Joshi, Solid State Commun. **34**, 65 (1980).
[26] K. W. Becker, S. Sykora, and V. Zlatic, Phys. Rev. B **75**, 075101 (2007).
[27] F. Wegner, Ann. Phys. **506**, 77 (1994).
[28] S. D. Głazek and K. G. Wilson, Phys. Rev. D **48**, 5863 (1993).
[29] S. D. Glazek and K. G. Wilson, Phys. Rev. D **49**, 4214 (1994).
[30] A. Hübsch and K. W. Becker, Eur. Phys. J. B **33**, 391 (2003).
[31] S. Sykora, A. Hübsch, and K. Becker, Eur. Phys. J. B **51**, 181 (2006).
[32] A. Hübsch and K. W. Becker, Phys. Rev. B **71**, 155116 (2005).
[33] P. Coleman, Phys. Rev. B **29**, 3035 (1984).
[34] S. Sykora, A. Hübsch, and K. Becker, Europhys. Lett. **76**, 644 (2006).
[35] P. W. Anderson, J. Phys. C **3**, 2436 (1970).
[36] S. K. Kehrein and A. Mielke, J. Phys. A **27**, 4259 (1994).
[37] P. Farkašovský, Phys. Rev. B **51**, 1507 (1995).
[38] P. Lemberger, J. Phys. A **25**, 715 (1992).
[39] N. W. Ashcroft and N. D. Mermin, *Solid State Physics* (Brooks-Cole, Belmont, 1976).
[40] R. Franco, M. S. Figueira, and M. E. Foglio, Phys. Rev. B **66**, 045112 (2002).